Atomic Spectroscopy

May/June 2017 Volume 38, No. 3

In This Issue:

ASPND7 38(3) 37 – 75 (2017)
ISSN 0195-5373

For subscriptions and/or articles see inside front cover.

Atomic Spectroscopy
Vol. 38(3), May/June 2017

Printed in the United States and published six times a year by:

PerkinElmer, Inc.
710 Bridgeport Avenue
Shelton, CT 06484-4794 USA
http://www.perkinelmer.com

SUBSCRIPTION INFORMATION

Atomic Spectroscopy
P.O. Box 3674
Barrington, IL 60011 USA
E-mail: atsponline@yahoo.com

2017 SUBSCRIPTION RATES

ORDER ON-LINE:
- pdf only -1 yr - U.S. $60.00
- 2 yr - U.S. $110.00
- pdf and printed copy -
  1 yr - U.S. $90.00
  2 yr - U.S. $160.00
- printed copy only -
  1 yr - U.S. $70.00
  2 yr - U.S. $130.00

PAYMENT BY CHECK:
Check must be drawn on U.S. bank in U.S. funds made out to: "*Atomic Spectroscopy*"

BACK CLAIMS/ADDRESS CHANGES:
- Subscriber claims for missing back issues will be honored at no charge within 90 days of issue mailing date.
  E-mail: atsponline@yahoo.com

ARTICLE INDEXING SERVICES
Thomson Reuters at:
www.scientific.thomsonreuters.com
Elsevier BV at:
www.elsevier.com

Guidelines for Authors

Atomic Spectroscopy serves as a medium for the dissemination of general information together with new applications and analytical data in atomic absorption spectrometry.

The pages of *Atomic Spectroscopy* are open to all workers in the field of atomic spectroscopy. There is no charge for publication of a manuscript.

The journal has around 1100 subscribers on a worldwide basis, and its success can be attributed to the excellent contributions of its authors as well as the technical guidance of its reviewers and the Technical Editors.

The original of the manuscript can be mailed to the editor in hard copy including electronic file on disk or CD (or simply by e-mail) in the following manner:

1. If mailed, provide text (double-spaced) and tables in hard copy plus on disk or CD with text and tables in .doc file; figures in doc or tif files.
3. Number the references in the order they are cited in the text.
5. Consult a current copy of *Atomic Spectroscopy* for format.
6. Editor's e-mail: anneliese.lust@perkinelmer.com or: annelieselust@aol.com

All manuscripts are sent to two reviewers. If there is disagreement, a third reviewer is consulted.

Minor changes in style are made in-house and submitted to the author for approval.

If a revision of the manuscript is required before publication can be considered, the paper is returned to the author(s) with the reviewers' comments.

In the interest of speed of publication, a pdf file of the typeset text is e-mailed to the corresponding author before publication for final approval.

Once the issue has been printed, each author receives a final pdf file of the article including 50 complimentary copies of the article and several copies of the complete issue.

Additional reprints can be purchased, but the request must be made before printing.

PerkinElmer. Inc., holds copyright to all material published in *Atomic Spectroscopy* unless otherwise noted on the first page of the article.

Anneliese Lust
Editor, *Atomic Spectroscopy*
PerkinElmer, Inc.
710 Bridgeport Avenue
Shelton, CT 06484-4794 USA

Direct Determination of Trace Lead in Seawater by Inductively Coupled Plasma Mass Spectrometry After Photochemical Vapor Generation

Shuzhen Li[a,c], Ying Gao[a,b,*], Ying Yu[b], Hongyan He[b], Xiaorong Hu[c], Shijun Ni[b], Zeming Shi[b], Xiuhong Peng[b], and Rui Liu[c]

[a] State Key Laboratory of Geohazard Prevention and Geoenvironment Protection, Chengdu University of Technology, Chengdu, Sichuan 610059, P.R. China

[b] College of Earth Sciences, Chengdu University of Technology, Chengdu, Sichuan 610059, P.R. China

[c] College of Materials and Chemistry & Chemical Engineering, Chengdu University of Technology, Chengdu 610059, P.R. China

ABSTRACT

A novel method is developed for the determination of lead in seawater samples using nickel-assisted photochemical vapor generation (PVG) coupled with inductively coupled plasma mass spectrometry (ICP-MS). The severe matrix effect of seawater on the suppression of the lead signal was efficiently eliminated by using a mixture of 15 μg g^{-1} Ni^{2+} and 10% (v/v) formic acid as a photochemical reduction medium, making direct determination of lead in seawater samples feasible. A method detection limit of 0.003 ng g^{-1} based on external calibration was obtained, and the sampling frequency of 20 h^{-1} was achieved with a 30-second sample loading time and a 1.25-mL sample consumption. The relative standard deviation of the measurement results was 3.7% (RSD, n=7) in seawater spiked with 1 ng g^{-1} Pb^{2+} solution. The proposed method was successfully applied for the analysis of one standard reference material (Seawater-QC3163) and three seawater samples (collected from Shanghai, Haikou, and Sanya, P.R. China) with satisfactory results.

INTRODUCTION

The presence of heavy metals poses a potential threat to marine ecosystems due to their toxicity, resistance to degradation, and consequent tendency to bioaccumulation (1, 2). Among them, lead (Pb) is toxic to humans, aquatic plants, and animals at trace levels (3-5) and is widely regarded as a good indicator of heavy metal pollution in marine environments caused by anthropogenic activities (6, 7). Elucidation of the distribution and concentration of lead in seawater is of great importance for identification of the contamination source and contamination prevention (1, 8, 9).

Atomic spectrometry-based techniques are the most popular methods for the determination of trace metals in environmental samples. Inductively coupled plasma mass spectrometry (ICP-MS) is one of the most powerful techniques due to its low detection limits, wide linear range, and high sample throughput (10, 11). However, direct determination of lead in seawater samples remains a challenge due to their extremely low concentrations and high salt matrix (12-14). Therefore, preconcentration and purification before detection is required for the analysis of lead in seawater. Solvent extraction and extraction onto chelating resin columns followed by atomic spectrometry detection were developed (15-17). But these methods are usually relatively labor-intensive (i.e., reagent purification and sample processing) and time-consuming as they often require large sample volumes (hundreds of milliliter to liter scale). A $Mg(OH)_2$ co-precipatation method with low procedural blank was also proposed for the determination of lead in seawater (18). Nevertheless, it could result in high content of sea salt in a sample matrix which can clog the nebulizer and leave deposits on the ICP-MS cones.

Chemical vapor generation (CVG) is a widely used sample introduction method for trace metal detection in atomic spectrometry which can greatly increase sample introduction efficiency and efficiently separate the analyte from its troublesome sample matrix (19). Conventional CVG methods often involve using high blank oxidation reagents and unstable reduction reagents, making it difficult to determine trace/ultra-trace concentrations of Pb in environmental samples. Purification of reagents before use or high purity reagents is always required (20, 21). Photochemical vapor generation (PVG), utilizing free radicals generated by photoredox reactions in the presence of low molecular weight organic compounds, not only remains the major advantage of CVG but also provides simpler reactions (22-24). For lead determination, metal ion-assisted PVG was developed for the analysis of sediments, soils, and river waters (25). In the presence of Ni^{2+}, a significant improvement in PVG efficiency of lead was achieved. The proposed method is simple, with low blanks compared to conventional CVG for lead, and avoids unstable reagents. However, the severe matrix effect is still a problem for the direct determination of

**Corresponding author.*
E-mail: ying.gaoy@gmail.com
Tel.: 86-28-8407-8773

lead in seawaters. The signal from Ni^{2+} was significantly suppressed in the presence of high concentrations of chloride, resulting in low PVG efficiency of Ni as well as a greatly decreased PVG efficiency of lead. Recently, Duan et al. (26) proposed a new method for the determination of trace lead by generating volatile lead species in the presence of 0.90% (v/v) acetic acid and 0.03% (v/v) hydrochloride acid under UV irradiatinon. This technique is simple, convenient, and has low blank. But the suppression effect of high concentration inorganic anions is also a problem for the direct analysis of seawater samples.

The purpose of this work was to develop a sensitive, simple, and direct method for the accurate determination of trace lead in seawater samples by nickel ion-assisted PVG coupled with ICP-MS detection. The accuracy of the proposed method is demonstrated by successful analysis of three seawaters.

EXPERIMENTAL

Instrumentation

An ELAN® DRC™-e ICP-MS (PerkinElmer, Inc., Shelton, CT, USA), equipped with quartz torch and alumina sample injector tube, was used. The fitted GemTip™ cross-flow nebulizer and a corrosion-resistant double-pass Ryton® spray chamber mounted outside the torch box were replaced by a PVG-system for lead determination. A model FIA-3110 flow injection pump system (Vital Instruments Co. Ltd., Beijing, P.R. China) was used for the introduction of sample solutions to the PVG system. A schematic of the UV-PVG photoreactor interfaced to the ICP-MS is similar to a previous report (25). The UV-PVG system consists of a 19 W thin film flow-through lamp (Beijing Titan Instruments Co., Beijing, P.R. China) loosely covered with aluminum foil to shield the operator from exposure to the UV. Argon carrier gas was introduced through a "T" connection between the outlet of the photoreactor and a tandem set of two homemade gas-liquid separators (GLSs, ~2 mL internal volume) maintained at 0 °C by immersion in an ice bath to minimize any transport of liquid droplets derived from condensation of water vapor to the ICP. The generated analyte vapors were directed from the outlet of the last GLS to the ICP-MS via a 0.25-m length of Teflon® lined Tygon® tubing. Optimization of the ICP-MS parameters was performed as recommended by the manufacturer. Optimum conditions for PVG were investigated independently. Typical operating conditions are summarized in Table 1.

Reagents and Standard Solutions

All reagents were of analytical reagent grade or better, and deionized water (DIW) was used throughout. ACS grade formic acid was obtained from Aladdin Industrial Corporation (Shanghai, P.R. China). Stock solutions of lead and nickel with the concentration of 1000 $\mu g\ g^{-1}$ were purchased from Environmental Express (South Carolina, U.S.). Lead working standard solution was prepared by dilution of the stock solution with 0.1% HCOOH. High-purity NaCl (trace SELECT, >99.999%) was obtained from Aladdin Industrial Corporation (Shanghai, P.R. China). A 2 M BrCl solution was prepared in a fume hood by dissolution of 27 g of reagent grade KBr (Fisher Scientific, Ottawa, Canada) in 2.5 L of HCl in a glass container, followed by slow addition of 38 g reagent grade $KBrO_3$ (Fisher Scientific, Ottawa, Canada). A rinse solution containing 0.04 M BrCl was prepared by dilution of the 2 M BrCl with deionized water (DIW) to efficiently eliminate any carry-over between the samples. A certified reference material QC3163 Seawater was obtained from Sigma Aldrich for method validation.

TABLE I
ICP-MS Instrumental Operating Parameters

Instrument Settings	ICP-MS
RF power	1175 W
plasma gas flow	15 L min^{-1}
Auxiliary gas flow	1.2 L min^{-1}
Nebulizer gas flow	1.0 L min^{-1}
Scanning mode	Peak hopping
Isotope monitored	^{208}Pb
Resolution	0.7 amu
Dwell time	30 ms
Dead time	50 ns
	UV-PVG
Sample flow rate	2.5 mL min^{-1}
Ar carrier gas flow rate to PVG	1.0 L min^{-1}

Three seawater samples were analyzed for method validation, which were collected from Sanya (Hainan, P.R. China), Haikou (Hainan, P.R. China), and Shanghai (Chongmingdao, P.R. China), respectively.

Standard Additions Sample Preparation and Analysis Procedure

For the determination of lead in seawater samples, standard addition calibration was applied. Three replicate subsamples of 10 g of each seawater sample were weighed into precleaned polyethylene bottles. A 10-g mass of a solution containing 20% formic acid (FA) and 0.3 g of a 1000-g g^{-1} Ni stock solution were added to each sample, resulting in a final concentration of 10% FA and 15 $\mu g\ g^{-1}$ Ni^{2+}. Appropriate amounts of the standard solution of Pb^{2+} were added to each spiked seawater sample to obtain approximately a 1-, 2-, and 4-fold increase in the Pb concentration, respectively. The unspiked and spiked samples were then diluted to 20 g with DIW.

Three sample blanks were prepared containing 10% FA, 15 μg g^{-1} Ni, and 1.75 % NaCl to match the matrix of the seawater samples. The sample solutions were subjected to UV-PVG-ICP-MS detection as described earlier. Briefly, the sample solution was quickly delivered to the PVG reactor at a sample flow rate of 2.5 mL min^{-1} and remained in the reactor for 50 seconds by stopping the pump for photochemical reduction of Pb into volatile species. Then the irradiated sample solution was transferred to the GLSs from the PVG reactor for analysis by ICP-MS at the same sample flow rate. For the next analysis, a solution of 0.04 M BrCl was used to efficiently rinse the system for 50 seconds to eliminate any carryover between the samples. The peak area of the ^{208}Pb isotope was used to construct a standard additions calibration curve for each sample.

RESULTS AND DISCUSSION

Serious suppression effects often occur when detecting metal ions in seawater samples by the PVG-based technique (27-29). According to the previous report, volatile species of Pb can be efficiently generated in 5% formic acid and 3 μg g^{-1} Ni^{2+} under UV irradiation (25). During initial experiments, a 5-ng g^{-1} Pb standard solution containing 5% formic acid, 3 μg g^{-1} Ni, and 1.75% NaCl (w/v) (matching matrix in the prepared seawater solutions) was introduced to the PVG reactor. The response from the solution was only 10% of that obtained from a matrix-free standard solution, showing the severe suppression effect of the sample matrix on lead detection in seawater samples. It was found that the PVG efficiency of Ni^{2+} was also significantly suppressed in the presence of high concentrations of chloride. It may be that the oxidative radicals generated from the sample matrix largely consumed the reductive radicals arising from photodecomposition of formic acid, resulting in the low PVG efficiencies of Ni and Pb. Increasing the concentration of formic acid could provide more available reductive radicals for the photochemical reduction of the analytes in seawater samples and potentially alleviate the effect of the seawater matrix. Due to the suppression effect of the sample matrix, spiked seawater instead of standard solution was used to investigate optimum PVG conditions for the determination of Pb.

Optimization of UV-PVG system

The formic acid concentration, Ni^{2+} concentration, UV irradiation time, and argon carrier gas flow rate comprised the four basic parameters which determined the PVG efficiency of the analyte and the transport efficiency to the ICP-MS. These parameters were investigated to obtain optimized responses on lead detection.

PVG efficiencies highly depend on the type and concentration of organic reductants used (28, 30-32). The effect of formic acid concentration in the range of 1%–40% (v/v) on the response (peak area normalized to the maximum achieved) of Pb in seawater spiked with 5 ng g^{-1} Pb solution is shown in Figure 1.

The signal response of ^{208}Pb increased with an increasing concentration of formic acid from 1% to 10% (v/v), and then decreased beyond 10%. Obviously, the optimum concentration of formic acid was higher than that of a previous report (5%, v/v). It suggests that reductive radicals arising from photodecomposition of formic acid were largely consumed by potentially oxidative radicals generated from the sample matrix, decreasing the available reductive radicals for the reduction of lead. Therefore, a higher concentration of formic acid was required for the efficient reduction of lead in seawater compared to that in a standard solution. But a further increase in concentration of formic acid above 10% (v/v) may lose penetration depth of the UV radiation into the sample as the absorption of the solution increases. In addition it may also increase possible side reactions or photodecomposition of the product and its redissolution in the aqueous phase. Consequently, 10% (v/v) formic acid was selected for subsequent measurement.

Metal ions play important roles for the reduction of Pb in a PVG system. The presence of Ni^{2+} in formic acid solution can significantly improve the PVG efficiency of Pb (25). Recently, ferric ion-

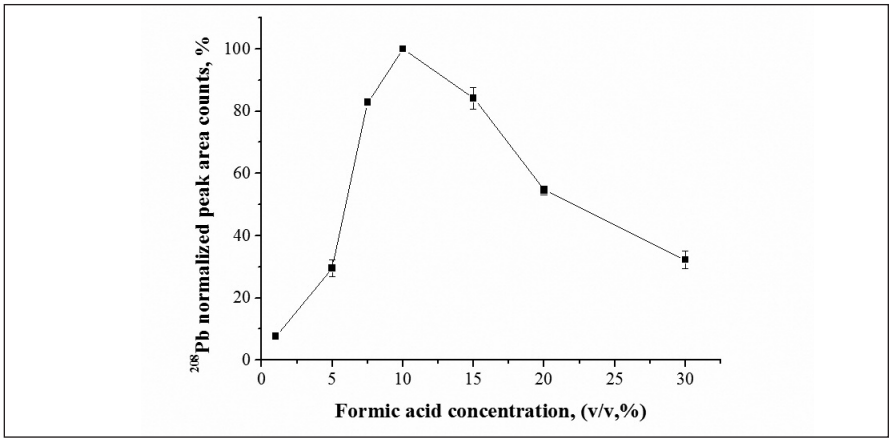

Fig. 1. The effect of formic acid concentration on lead detection.

induced enhancement of PVG was also observed for As detection (33). The effect of added Ni^{2+} concentration in the range of 0–30 μg g^{-1} on the response (peak area normalized to the maximum achieved) of Pb in seawater spiked with 5 ng g^{-1} Pb solution is shown in Figure 2. The peak area of ^{208}Pb increased with an increase in Ni^{2+} concentration from 0 μg g^{-1} to 15 μg g^{-1}, followed by a slight decrease at higher concentrations. The optimal concentration of Ni^{2+} for the efficient generation of volatile Pb in seawater was five times higher than that obtained from standard solution, which was likely owing to the severe suppression of the generation of volatile Ni^{2+} in the presence of high concentrations of Cl^-. Although the mechanism of metal-ion-assisted PVG reaction was not clear, the generation of significant amounts of volatile Ni species were needed to enhance charge transfer reactions of Pb and to facilitate the reduction of Pb. Therefore, 15 μg g^{-1} Ni^{2+} was selected for all subsequent measurements.

The dosage of UV radiation received by sample solution mainly determines the efficiencies of radical formation and the vapor generation of lead. The effect of UV irradiation time over the range of 30–150 seconds was investigated using seawater spiked with 5 ng g^{-1} Pb containing 10% formic acids and 15 μg g^{-1} Ni^{2+}. As shown in Figure 3, the responses initially sharply increased as irradiation time increased from 30 to 50 seconds. Thereafter, a quick decrease occurred with a further increase in irradiation time. The relatively short irradiation time leads to inefficient generation of volatile Pb species, and with increased irradiation time leads to the reoxidation of volatile Pb species by photo-decomposed oxidative radicals from the sample matrix. The optimal UV irradiation time of Pb in seawater samples was much less than reported previously (25). This probably is due to the combined effect of sample matrix and the air temperature around the UV lamp. After UV irradiation with 50 seconds at room temperature (25 °C), the temperature of the sample solution through the UV reactor was nearly 60 °C. When a mini-fan was set under the UV reactor to accelerate circulation of air around the UV lamp, the optimal UV irradiation time was delayed to 100 seconds. Furthermore, the temperature of the sample solution after 50 seconds irradiation was down to 48 °C, which suggested that the air temperature around the UV lamp influenced the kinetics of PVG for Pb. Therefore, an irradiation time of 50 seconds (at 25 °C) was selected for all subsequent measurements to achieve a maximum response and reasonable sample throughput.

The argon carrier gas flow rate through GLS influences the liquid gas separation efficiency of the volatile Pb species as well as the depth of sampling in the plasma. The effect of argon carrier gas flow rate on the response of Pb from spiked seawater was optimized in the range of 0.8–1.1 L min^{-1}. As shown in Figure 4, maximum response was obtained at the 1.0 L min^{-1} gas flow rate. Lower carrier gas flow rates may lead to inefficient stripping and transport of the analyte from the solution to the ICP-MS; whereas higher flow rates will result in significant dilution of the analyte in the carrier gas. Therefore, the Ar carrier gas flow rate to the GLS of 1.0 L min^{-1} was selected for all subsequent measurements.

Figures of Merit

Under optimal experimental conditions, the signal response of lead from 1.75% NaCl (w/v) (matching the matrix in the prepared seawater solution) was approximately 90% of that from the same concentration of the matrix-free standard solution

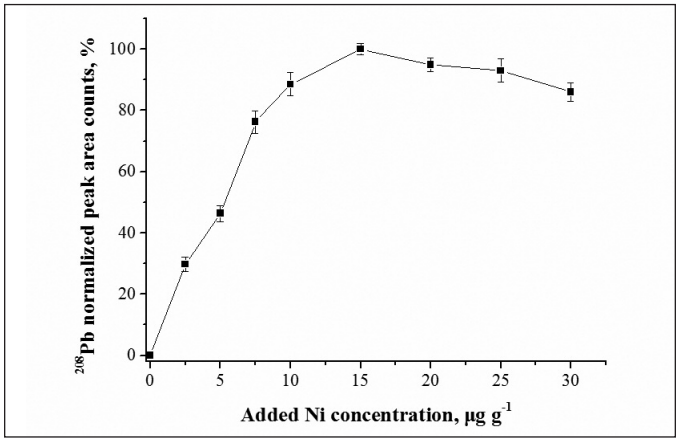

Fig. 2. The effect of Ni^{2+} concentration on lead detection.

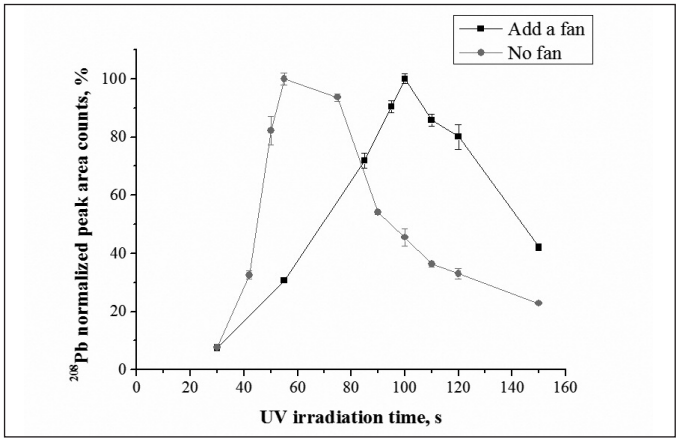

Fig. 3. The effect of UV irradiation time and temperature on lead detection.

with 5% formic acid and 3 μg g^{-1} Ni^{2+}. A relatively good precision of 3.7% RSD was obtained from the replicate measurements of the seawater samples spiked with 1 ng g^{-1} Pb (n = 7). The sampling frequency of 20 h^{-1} was achieved with a 30-second sample loading time and a 1.25-mL sample consumption for each analysis. Good linear response was obtained from Pb standard solutions prepared in the range of 0.02–200 ng g^{-1} in 1.75% NaCl. A method detection limit of 0.003 ng g^{-1} was obtained using external calibration, based on three times the standard deviation of the analyte concentration arising from the method blank which comprises a solution of 1.75% NaCl, 10% formic acid, and 15 μg g^{-1} of Ni^{2+} in DIW (see Figure 5). Compared to photo-CVG-MC-ICP-MS determination, the LOD is slightly improved, which is 0.005 ng g^{-1}. It is probably due to the better measurement precision of MC-ICP-MS. But it is 30 times lower than with the direct solution nebulization method after 10-fold dilution prior to analysis (0.09 ng g^{-1}) for the analysis of seawater samples (Table II). Also, the proposed method is more sensitive than most of the traditional methods with the HG technique, and is comparable with methods by ICP-MS detection after solid phase extraction. In addition, the method blank can be easily controlled as per the latest report for Pb detection by the PVG method (26). But this method has great advantages for the direct analysis of seawater samples.

Pb Determination in Seawater

To compensate for matrix effects and achieve accurate results, standard additions were used for seawater analysis. Three seawater samples were analyzed under optimal experimental conditions. Seawater solutions with gravimetric additions of approximately 1-, 2-, and 4-fold the endogenous Pb content were prepared, yielding a calibration curve with a correlation coefficient greater than 0.999. The analytical results are listed in Table III.

TABLE II
Comparison of LODs for Pb Using Different Techniques

Chemical Reagents	Method	Preconcentration	Samples	LOD	Ref.
-	ICP-MS	PVC-packed mini-column	Seawater	7 pg g^{-1}	(14)
-	ICP-OES	Ionic imprinted polymer	Seawater	1.88 ng g^{-1}	(16)
0.28 mol L^{-1} H_2O_2, 0.1 mol L^{-1} HNO_3, and 1.5% (m/v) $NaBH_4$	HG-ICP-MS	-	Seawater	0.024 ng g^{-1}	(34)
1% (v/v) HCl, 2% (m/v) $K_3Mn(CN)_6$, and 2% (m/v) $NaBH_4$	HG-ICP MS	-	Seawater	0.008 ng g^{-1}	(21)
0.90% acetic acid (v/v) and 0.030% HCl (v/v)	PVG-ICP-MS	-	Tap Water and Lake Water	0.0036 ng g^{-1}	(26)
15 μg g^{-1} Ni^{2+} and 10% (v/v) formic acid	PVG-ICP-MS	-	Seawater	0.003 ng g^{-1}	This work

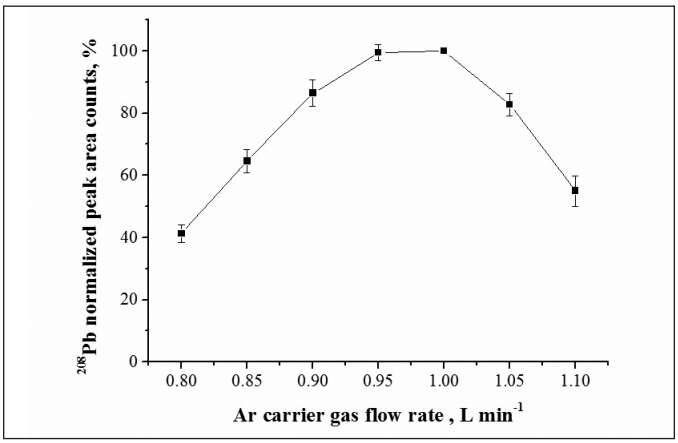

Fig. 4. The effect of Ar carrier gas flow rate on lead detection.

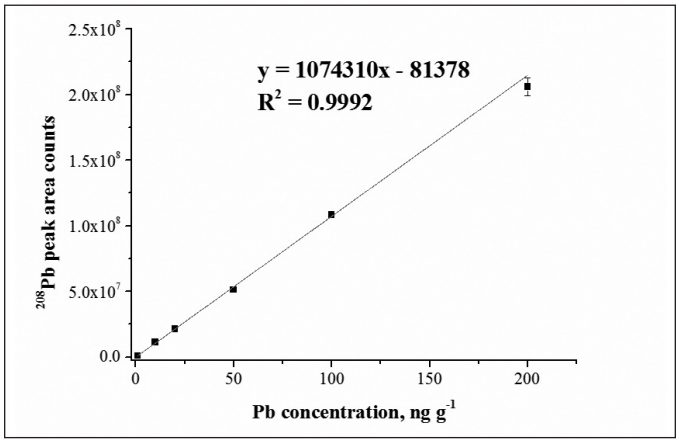

Fig. 5. PVG calibration curve generated from standard solutions containing 1.75% NaCl, 10% formic acid, and 15 μg g^{-1} Ni^{2+}.

TABLE III
Determination of Pb in Seawater

Sample and Method	Determined ng g^{-1} (SD, n = 3)	Spiked Value ng g^{-1} (SD, n = 3)	Spike Recoveries (%)
Sanya (Std. Add.)	0.26 ± 0.04	0.30	108.9 ± 8.0
Haikou (Std. Add.)	0.14 ± 0.01	0.30	106.2 ± 7.7
Shanghai (Std. Add.)	1.29 ± 0.02	1.00	95.2 ± 1.6

TABLE IV
PVC-ICP-MS Determination of Pb in a Certified Seawater Sample

Sample	Determined ng g^{-1} (SD, n = 3)	Certified ng g^{-1} (k=2)
QC3163 Seawater	691 ± 17.8	693 ± 6.4

To further demonstrate the analytical accuracy of this method, the spiked recovery test was applied. The recoveries of spiking 0.3 ng g^{-1} and 1.00 ng g^{-1} of Pb into the seawater samples were in the range of 95.2–108.9%. The developed method was also applied for the analysis of a certified seawater sample. The analytical result is shown in Table IV and is in agreement with the certified values, confirming the accuracy of the proposed methodology.

CONCLUSION

A novel and sensitive approach is developed for the direct determination of Pb in seawaters using nickel-assisted PVG for sample introduction with ICP-MS detection. The severe matrix effect from seawater was efficiently eliminated by using 10% (v/v) formic acid and 15 μg g^{-1} Ni^{2+} as the photochemical reductant medium, making direct determination of Pb in seawater feasible. The method provides a detection limit of 0.003 ng g^{-1} for Pb using external calibration, suitable for ultratrace determinations of Pb in seawaters. The proposed method has promising application for the determination of trace Pb in seawater samples.

ACKNOWLEDGMENT

Sichuan Youth Science and Technology Foundation (No. 2017JQ0043), China Postdoctoral Science Foundation (No. 2016M590870), State Key Laboratory of Geohazard Prevention and Geoenviroment Protection Independent Research Project (SKLGP2016Z006), the Education Department of Sichuan Province (Grant No. 17ZA0040) and the Cultivating Program of Middle-aged Backbone Teachers Program of Chengdu University of Technology (Grant No. KYGG201409) are acknowledged for their financial support. The authors declare no competing financial interest.

Received January 11, 2017.

REFERENCES

1. C. Christophoridis, D. Dedepsidis, and K. Fytianos, J. Hazard. Mater. 168, 1082 (2009).
2. Y. Dong, R.K. Rosenbaum, and M.Z. Hauschild, Environ. Sci. & Technol. 50, 269 (2016).
3. K. Chen, L. Huang, B. Yan, H. Li, H. Sun, and J. Bi, Environ. Sci. & Technol. 48, 12930 (2014).
4. D. Absalon and B. Slesak, Science of the Total Environment 408, 4420 (2010).
5. R.L. Boeckx, Anal. Chem. 58, 274A (1986).
6. Y. Li, R.J. Yang, A.B. Zhang, and S.R. Wang, Mar. Pollut. Bull. 85, 700 (2014).
7. M. Komarek, V. Ettler, V. Chrastny, and M. Mihaljevic, Environ. Int. 34, 562 (2008).
8. M.F. Soto-Jimenez, F. Paez-Osuna, G. Scelfo, S. Hibdon, R. Franks, J. Aggarawl, and A.R. Flegal, Marine Environmental Res. 66, 451 (2008).
9. J.F. Wu and E.A. Boyle, Geochim. Cosmochim. Acta 61, 3279 (1997).
10. S. Hill, Inductively Coupled Plasma Spectrometry and its Application, Blackwell Publishing, Oxford, UK, 98 (2007).
11. W. Xu, S.J. Ni, Y. Gao, and Z.M. Shi, Spectrosc. Lett. 48, 542 (2015).
12. J.M. Lee, E.A. Boyle, Y. Echegoyen-Sanz, J.N. Fitzsimmons, R.F. Zhang, and R.A. Kayser, Anal. Chim. Acta 686, 93 (2011).
13. D.V. Biller and K.W. Bruland, Mar. Chem. 130, 12 (2012).
14. C.K. Su, T.W. Lee, and Y.C. Sun, J. Anal. At. Spectrom. 27, 1585 (2012).
15. J.E. O'Sullivan, R.J. Watson, and E.C.V. Butler, Talanta 115, 999 (2013).
16. N. Garcia-Otero, C. Teijeiro-Valino, J. Otero-Romani, E. Pena-Vazquez, A. Moreda-Pineiro, and P. Bermejo-Barrera, Anal. Bioanal. Chem. 395, 1107 (2009).
17. T. Minami, W. Konagaya, L.J. Zheng, S. Takano, M. Sasaki, R. Murata, Y. Nakaguchi, and Y. Sohrin, Anal. Chim. Acta 854, 183 (2015).
18. D. Weiss, E.A. Boyle, V. Chavagnac, M. Herwegh, and J.F. Wu, Spectrochim. Acta Pt. B, At. Spectrosc. 55, 363 (2000).
19. Y. Gao, R. Liu, and L. Yang, Chin. Sci. Bull. 58, 1980 (2013).
20. K. Huang, H. Xia, M. Li, Y. Gao, C. Zheng, and X. Hou, Analytical Methods 4, 4058 (2012).

21. V. Yilmaz, Z. Arslan, and L. Rose, Anal. Chim. Acta 761, 18 (2013).

22. X. Guo, R.E. Sturgeon, Z. Mester, and G.J. Gardner, Anal. Chem. 76, 2401 (2004).

23. Y. Yin, J. Liu, and G. Jiang, Trac-Trends in Anal. Chem. 30, 1672 (2011).

24. C. Zheng, Q. Ma, L. Wu, X. Hou, and R.E. Sturgeon, Microchem. Journal 95, 32 (2010).

25. Y. Gao, M. Xu, R.E. Sturgeon, Z. Mester, Z. Shi, R. Galea, P. Saull, and L. Yang, Anal. Chem. 87, 4495 (2015).

26. H.L. Duan, N.N. Zhang, Z.B. Gong, W.F. Li, and W. Hang, Spectrochim. Acta Part B, At. Spectrosc.120, 63 (2016).

27. X.M. Guo, R.E. Sturgeon, Z. Mester, and G.J. Gardner, Anal. Chem. 75, 2092 (2003).

28. Y. Gao, R.E. Sturgeon, Z. Mester, X. Hon, C. Zheng, and L. Yang, Anal. Chem. 87, 7996 (2015).

29. Y. Gao, R.E. Sturgeon, Z. Mester, X. Hou, and L. Yang, Anal. Chim. Acta 901, 34 (2015).

30. Y. Zeng, C. Zheng, X. Hou, and S. Wang, Microchem. Journal 117, 83 (2014).

31. H.L. Duan, Z.B. Gong, and S.F. Yang, Journal of Anal. At. Spectrom. 30, 410 (2015).

32. R.E. Sturgeon, Anal. Chem. 87, 3072 (2015).

33. Y.L. Wang, L.L. Lin, J.X. Liu, X.F. Mao, J.H. Wang, and D.Y. Qin, Analyst 141, 1530 (2016).

34. P.K. Petrov, G. Wibetoe, and D.L. Tsalev, Spectrochim. Acta Part B, At. Spectrosc. 61, 50 (2006).

Detection of *Shigella flexneri* DNA by ICP-MS Based on Oligonucleotide Hybridization and Labeling of Gold Nanoparticles

Xiuji Wang[a,b], Lanlan Jin[a], Wei Guo[a], Liuqin Huang[a], and Shenghong Hu[a,*]
[a] State Key Laboratory of Biogeology and Environmental Geology, School of Earth Sciences, China University of Geosciences, Wuhan, 430074, P.R. China
[b] Center of Analysis, Guangdong Medical University, Dongguan, 523808, P.R. China

ABSTRACT

A simple and sensitive detection method to target DNA of *Shigella flexneri* was developed by quantification of gold nanoparticles (AuNPs) using inductively coupled plasma mass spectrometry (ICP-MS). A sandwich hybridization assay was established to identify the target DNA using biotinylated capture probes and AuNP-labeled reporter probes in microfuge tubes. The hybridized products were immobilized on microplates via biotin-streptavidin affinity, and subsequently separated with excess non-hybridized probes by washing. Au, originating from the hybridized compounds, was detected by ICP-MS. Good linearity was obtained between the concentration of the target DNA and ^{197}Au signal intensity. The limit of detection (LOD, 3σ) for the target single-stranded DNA (ssDNA) and the simulated target double-stranded DNA (dsDNA) was calculated as 0.39 pM and 39.17 pM. The relative standard deviation (RSD, n = 3) for 10 pM target ssDNA was found to be 5.8%. The advantages of the proposed method include convenient separation of the hybridization compounds by the biotin-streptavidin system, ease of acquiring reporter probes labeled with AuNPs, and high sensitivity as a DNA assay.

INTRODUCTION

The sensitive detection of DNA is very important in the fields of disease diagnosis, food safety, and environmental monitoring because the genus of bacteria, viruses, and other microorganisms contribute to human diseases. Various molecular methods based on nucleic acid technologies (1, 2) have been developed in which sequence-specific DNA oligonucleotides (DNA probes) are used directly in hybridization assays or as primers in amplification reactions to determine the specific target DNA related to pathogenic microorganisms. Polymerase chain reaction (PCR) based on the design of primers, especially real-time PCR, has been developed for DNA quantification and has shown high sensitivity and specificity because of amplification (3–5). However, the complicated design of primers has unavoidably limited the application of this kind of method (6). The sequence-selective DNA detection methods based on hybridization assays rely on thermolecular recognition abilities of the DNA probes that hybridize with their complementary sequences. Target nucleic acids are quantified on the basis of the chemical nature of tags attached to DNA probes. Commonly, DNA probes are labeled frequently with radioactive agents (7, 8), fluorescent tags (9, 10), and chemiluminescence reagents (10, 11). However, some disadvantages, such as safety concerns and disposal problems of radioactive agents, sophisticated synthesis and spectral overlap of fluorescent tags, significantly limit their application in DNA quantification.

Recently, inductively coupled plasma mass spectrometry (ICP-MS) based on element tag and hybridization has been used as a complementary technique for the targeted analysis of nucleic acids. In the hybridization assays, the capture probes and the reporter probes labeled with element tags are specifically complementary to the target DNA sequence. After the hybridization products are anchored to the surface of magnetic beads or microplates by capture probes, elements from the reporter probes bound to the hybridization products can be quantified by ICP-MS. Two kinds of elements, lanthanide chelates or metal nanoparticles (gold or silver), are commonly used as tags to label biomolecules and the specific activities of biomolecules can be retained after modification. Lanthanide elements can be tagged to biomolecules using the same strategy because of their similar properties, which favors multiplex analysis (12, 13). Nanoparticles are another useful elemental tag for their easy preparation and the enhanced signal from nanoparticles containing numerous metal atoms (14–16). Gold nanoparticle-based probes have been used in the determination of DNA. Han et al. (17) presented an effective and ultrasensitive method for a one-step homogeneous DNA assay using single-nanoparticle detection by ICP-MS. Multiplex quantification of DNA targets associated with clinical diseases [human immunodeficiency virus (HIV), hepatitis A virus (HAV), and Hepatitis B virus (HBV)] were reported by labeling the probes with different NPs (Au NPs, Ag NPs, and Pt NPs) and detecting hybridizations using single-particle (SP) ICP-MS (18). In conclusion, methods based on ICP-MS for the determination of nucleic acids cannot only achieve multiplex analysis

**Corresponding author.*
E-mail: shhu@cug.edu.cn

easily, but also quantify lower abundance DNA targets without PCR amplification because of its low detection limit for metal elements. This kind of method provides a more precise and sensitive signal of the mass-to-charge ratios from the labeled element (especially nanoparticles) of the DNA probe and alleviates the time-consuming and labor-intensive work (6, 19).

Infections caused by *Shigella flexneri* are important agents of diarrhea and dysentery (20-22). In this study, we present a new approach to quantify a 28-base conserved DNA sequence of *Shigella flexneri* using a hybridization assay combined with ICP-MS as the detection technique. The synthesized specific target DNA associating with the *Shigella flexneri* was identified by the reporter probes labeled with AuNPs and the capture probes in a sandwich hybridization assay. The intensities of ^{197}Au were obtained using ICP-MS after the hybrid complexes were separated by the biotin-streptavidin affinity reaction and dissolved in 5% HNO_3. This is the first report of ICP-MS used to determine the specific genomic sequence of *Shigella flexneri*. Optimization of the hybridization assay, concentration of streptavidin coated on the microwell, specificity of hybridization, and the analytical performance are also described.

EXPERIMENTAL

Instrumentation

A 7700x series ICP-MS (Agilent Technologies Inc., Tokyo, Japan) was used in detecting the ^{197}Au signal. A solution of 100 ng g^{-1} ^{103}Rh internal standard was spiked into all samples. The optimized parameters for ICP-MS are listed in Table I. A JEM-2010 transmission electron microscope (TEM) (Philips CM12 TEM/STEM, The Netherlands) was used to characterize the AuNPs. A UV-1750 spectrophotometer (Shimadzu, Suzhou, P.R. China) was used for recording the ultraviolet-visual (UV-Vis) absorption spectrum of the AuNPs and the reporter probes labeled with the AuNPs in a 1-cm quartz cell.

Reagents and Materials

All oligonucleotides and DNA probes were synthesized by Shanghai Sangon Biotech Co., Ltd. (Shanghai, P.R. China). The sequences of the oligonucleotides used in this study are listed in Table II (see page 48) where Sequence 3 was target ssDNA, Sequence 7 was the complementary strand to target ssDNA, and others were mismatched oligonucleotides. All of these were dissolved in ultrapure H_2O. The capture probe (Sequence 1) and the reporter probe, functionalized with the thiol groups (−SH) at the 3'-end (Sequence 2), was diluted in the TE buffer.

The streptavidin was obtained from Shanghai Sangon Biotech Co., Ltd. Bovine serum albumin (BSA) was purchased from Wuhan Chu Cheng Zheng Mao Science and Technology Engineering Co. Ltd. (Wuhan, P.R. China). Chloroauric acid ($HAuCl_4 \cdot 4H_2O$) for AuNPs preparation was acquired from Sinopharm Chemical Reagent Co. Ltd. (Shanghai, P.R. China). Tween 20 was purchased from Sigma–Aldrich Chemical Co. (St. Louis, MO, USA).

TABLE I
Operating Parameters for ICP-MS

Parameters	Description
ICP RF power	1450 W
Plasma gas flow rate	15 L min^{-1}
Carrier gas flow rate	1.02 L min^{-1}
Auxiliary gas flow rate	1.0 L min^{-1}
Sample uptake rate	0.35 mL min^{-1}
Integration time	1.5 s
Sampling depth	8 mm
Replicates	3
Isotope used	^{197}Au
Internal standard used	^{103}Rh

The buffers and solutions used were (a) phosphate buffered saline (PBS, pH 7.4); (b) coating buffer: (Na_2CO_3, $NaHCO_3$, pH 9.6); (c) blocking buffer: 5% BSA in PBS; (d) hybridizing buffer (PBS, pH 7.8); (e) washing solution (PBS, Tween 20 0.04%, pH 7.4); and (f) TE buffer: 10 mM Tris-HCl, 1 mM EDTA, pH 8.0. All buffers were prepared using ultra-pure water (18.2 $M\Omega\ cm^{-1}$).

Preparation of Reporter Probes Modified by AuNPs

Gold particles, approximately 15 nm,. were synthesized according to previously published procedures (23, 24). For subsequent experiments, the solution was diluted to 50 mL with ultrapure water. The average particle diameter of about 15 nm was measured using TEM, which is shown in Figure 1(a). The final concentration of gold particles could be estimated using Beer's Law by using the extinction coefficient of about $10^8\ M^{-1}\ cm^{-1}$ for 15-nm diameter particles at around 520 nm (24).

The preparation of reporter probes modified by AuNPs was performed according to the literature (18, 25). The DNA probes, modified with AuNPs, were adjusted to a stock concentration of 0.2 M sodium and 0.1 M phosphate buffer (pH=7.0) for subsequent use. The UV–Vis spectra of the 15 nm AuNPs and the AuNPs conjugated with reporter probes are shown in Figure 1(b). The results showed a 5-nm red-shift. This was caused by the increase in size of the AuNPs when conjugated to the ssDNA, thus confirming the attachment of the ssDNA to the NPs (26).

Hybridization Assay

Before the hybridization assay, micro-well plates were coated with

streptavidin. One hundred microliters of streptavidin (diluted 100x with coating buffer) was added into each well and incubated at 4 °C overnight. After washing twice with PBST, the coated micro-well plate was blocked using a blocking buffer at 37 ºC for 2 hours. The schematic diagram of the hybridization assay is shown in Figure 2. An artificial 28-base oligonucleotide (Sequence 3) was used in its single-stranded form as the specific target DNA which was a conserved sequence of *Shigella flexner*i. Initially, a 10-µL solution of target ssDNA (Sequence 3), 10 µL of biotinylated capture DNA (Sequence 1), and 20 µL of hybridizing buffer were mixed in a microfuge tube and hybridized for 20 minutes at room temperature. Then, 5 µL of the reporter probes (Sequence 2) labeled with AuNPs was added into each tube and incubated for another 20 minutes at room temperature. The hybridized products were transferred into the coated microplates to be incubated at 37 ºC for 30 minutes before being washed three times by PBST and twice by ultra-pure water. A 5% (v/v) HNO_3 solution was added to release AuNPs from the hybridized complexes, and the ^{197}Au intensities were determined using ICP-MS. External calibration was used for the quantitative determination of the target ssDNA.

Simulated target dsDNA sequences were obtained by mixing the equimolar ratio of Sequence 3 and Sequence 7 in water (27). The solution was first boiled at 95 ºC for 5 minutes to melt the duplex and then cooled slowly to room temperature. A 10-microliter solution of capture DNA probes (Sequence 1), 10 µL of reporter probes functionalized with AuNPs, and 20 µL hybridization buffer were added to the dsDNA solution and incubated for 30 minutes. Subsequent steps followed the same procedure as that for the target ssDNA. All experiments were performed in triplicate.

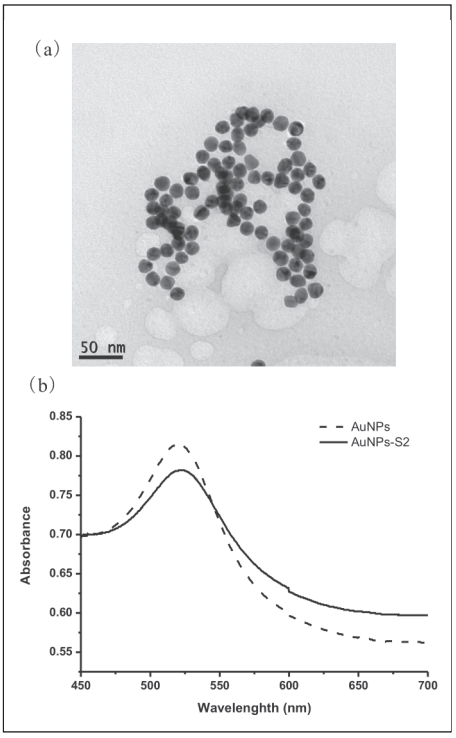

Fig. 1 (a and b). (a) TEM image of 15-nm gold nanoparticles (AuNPs) and (b) Ultraviolet-visual spectrum of synthesized AuNPs, and AuNPs conjugated with reporter probes (S2, Sequence 2).

RESULTS AND DISCUSSION

Optimization of the Hybridization Assay Conditions

A sandwich hybridization is presented in the schematic diagram (Figure 2). First, the excess capture DNA probes were reacted with the target ssDNA in hybridization 1. Then, the hybridized complexes were reacted with the reporter probes labeled with AuNPs in hybridization 2. The sensitivity of this assay is dependent on the number of hybridized complexes that are bound to the microplates via biotin-streptavidin affinity. More sites would be occupied by excess-free biotin-labeled capture probes, and fewer hybrids complexed with capture probes would be immobilized by the microplate, which might result in poor detection sensitivity and reproducibility. In addition, an excess of reporter probes labeled with AuNPs in the reaction system is essential for hybridization; however, a high concentration of reporter probes would lead to high background intensity (28). Therefore, the hybridization conditions should be optimized to increase the detection sensitivity.

A series of capture probes (Sequence 1) were investigated to identify an appropriate concentra-

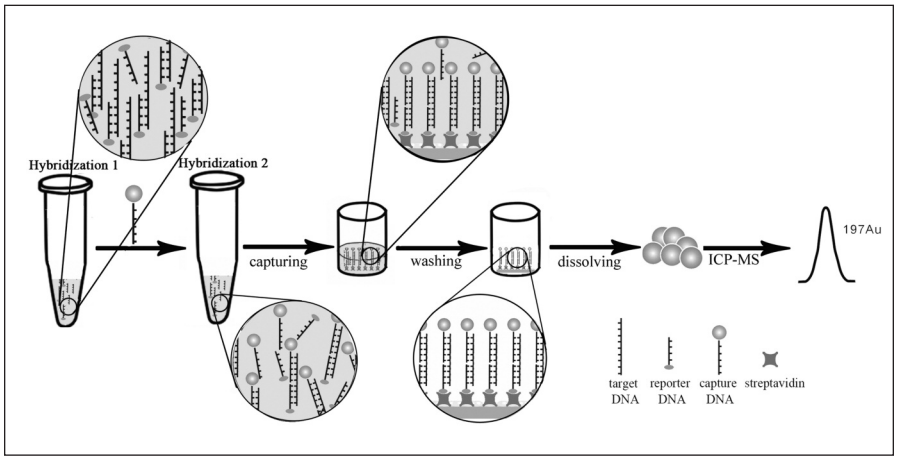

Fig. 2. Schematic diagram of the assay to detect DNA based on oligonucleotides hybridization and the quantification of gold nanoparticles (AuNPs) by ICP-MS.

tion when the target ssDNA was 10 pM and the dilution ratio of the reporter probes labeled with AuNPs was 1:10. The Au signal intensities were acquired when the concentration of Sequence 1 changed from 0.01 to 5 nM. As shown in Figure 3(a), the highest ratio of Au signal/background intensity appeared when the concentration was 0.5 nM. Therefore, 0.5 nM of Sequence 1 was used for subsequent hybridizations.

The dilution ratio of reporter probes labeled with AuNPs was optimized from 1:2 to 1:50 with a target ssDNA concentration of 10 pM. Figure 3(b) shows that a favorable ^{197}Au signal/background ratio was obtained until the dilution ratio of the probes was reduced 1:20. According to the results, a higher dilution of the Au NPs-modified probes when hybridizing with the target DNA might result in poorer detection sensitivity, while a lower dilution ratio would probably result in a higher background and poorer detection sensitivity. Consequently, a 1:20 dilution of AuNPs-modified probes was selected to be applied in the hybridization assay considering both the effect of detection sensitivity and background.

Effect of Streptavidin Concentration on Au Signal/Background Ratio

A convenient system for separating hybridization complexes from other reagents was carried out by microplates coated with streptavidin. In this system, streptavidin was used to fix hybridization by the capture DNA because streptavidin binding to biotin is specific enough to ensure that the binding is directed only to the target of interest (29). The concentration of streptavidin coated on the microplate was a key factor for the Au signal/background intensity ratio. The dilution ratio of streptavidin (1 mg mL^{-1}) from 1:50 to 1:200 was investigated when the target ssDNA was in the range from 0.5 to 50 pM. Figure 4 indicates that the same results were obtained with a dilution ratio of 1:50 and 1:100. The latter was appropriate for further studies because less streptavidin was consumed.

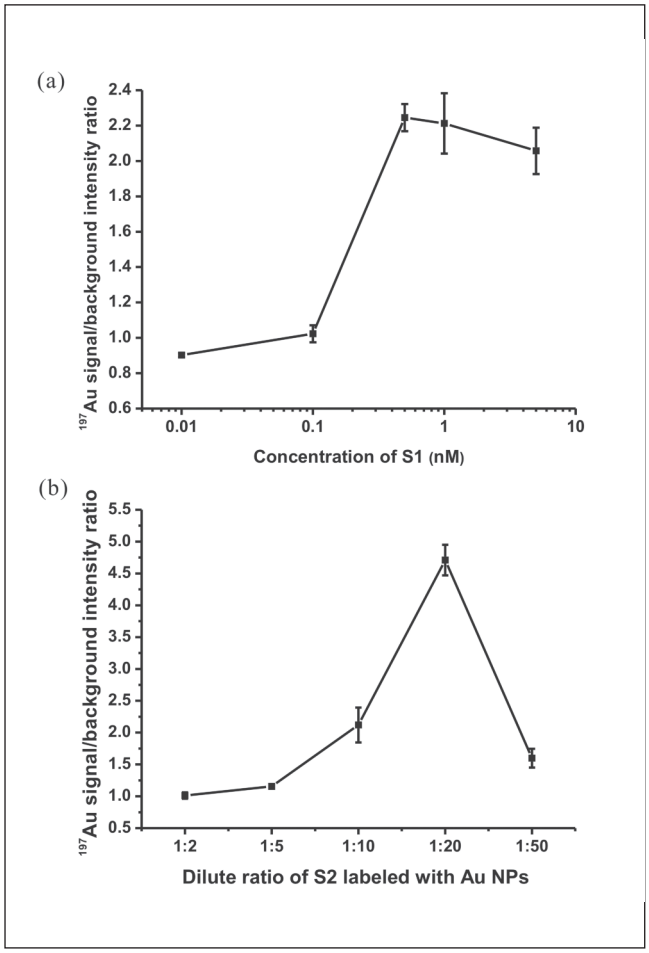

Fig. 3 (a and b). Effect of (a) concentration of capture DNA probes (S1, Sequence 1) and (b) dilution ratio of reporter probes (S2, Sequence 2) on the Au signal/background ratio. Target ssDNA was at a concentration of 10 pM.

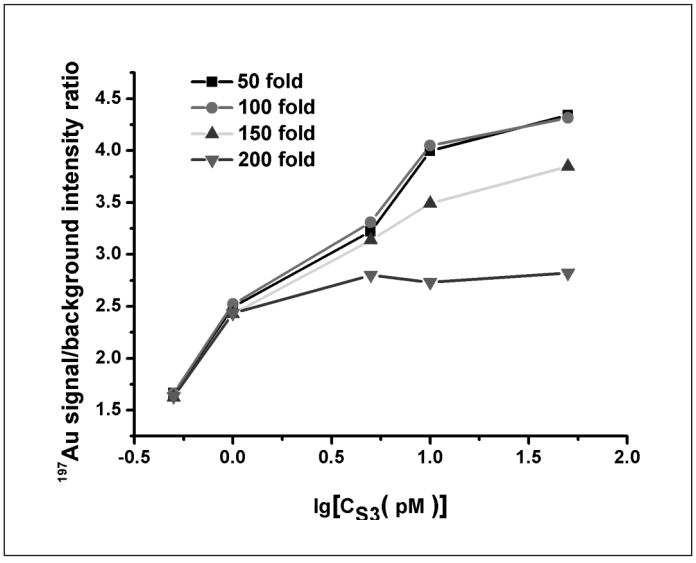

Fig. 4. Effects of concentration of streptavidin on the ^{197}Au signal/background ratio.

Specificity of Hybridization

In the detection of *Shigella flexneri* in environmental or clinical samples, thousands of other mismatched and random length DNA fragments are present in the DNA lysate together with the target DNA. To verify specificity of hybridization, three mismatched ssDNA sequences were also tested using the same experimental procedure (Figure 5). Sequence 4 had a 1-base mismatch oligonucleotide, and Sequence 5 had a 5-base mismatch oligonucleotide, respectively, while Sequence 6 was a random oligonucleotide sequence (Table II). Compared to other mismatched and the random DNA sequences, a higher intensity of ^{197}Au from the completely matched target DNA (Sequence 3) was observed, which indicated that the target DNA could be distinguished easily in the presence of other irrelevant sequences using this method.

Analytical Performance

This method was based on the indirect detection of synthetic target DNA sequences of *Shigella flexneri* in a proof-of-principle experiment. The artificial target ssDNA was studied first. Under the optimized conditions, a series of concentrations of the target ssDNA sequence, from 0.5 to 50 pM, was tested in the quantitative assay. As shown in Figure 6(a), the signal intensity of ^{197}Au correlated linearly with the logarithm of the target DNA concentration (correlation coefficient of r^2=0.9715). The precision for concentration of the target DNA at 10 pM with three replicate measurements was 5.8% (RSD). The detection limit (LOD, 3σ) of the proposed method for the 28-base synthesized target ssDNA was calculated to be 0.39 pM, where the σ is the standard deviation of repetitive measurements of the assay solution blank.

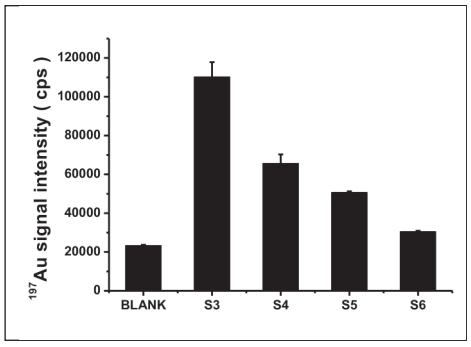

Fig. 5. Specificity for the determination of target ssDNA (S3, Sequence 3) using the proposed hybridization (S4, Sequence 4; S5, Sequence 5; S6, Sequence 6). All oligonucleotides were used at a concentration of 1 pM.

TABLE II
Sequences of Oligonucleotides Used in DNA Hybridization

Name	Sequence (5'–3')
Sequence 1	Biotin-gcagtCCGAAGTTAAGCTAC
Sequence 2	CTACTTCTTTTAC-$(CH2)_6$-SH
Sequence 3	GTAAAAGAAGTAGGTAGCTTAACTTCGG
Sequence 4	GTAAAAGCAGTAGGTAGCTTAACTTCGG
Sequence 5	GTGGGAGAAGCCGGTAGCTTAACTTCGG
Sequence 6	ACATCTGCATTTCCGTTAAAGTCCCGTTCGTAAATGCTGTT-GCGGCTTGCTTTTCCGCG
Sequence 7	CCGAAGTTAAGCTACCTACTTCTTTTAC

DNA is not readily available to bind complementary sequences in its native form because it is usually present as a double-strand molecule in organisms. Thus, it is necessary to convert dsDNA to ssDNA by melting the duplex before hybridization. In this process, the probes and the degraded complementary sequences were competitively combined with the target ssDNA (30). Compared with the spiked target ssDNA, quantifying the dsDNA required the addition of excess reporter DNA probes (Sequence 2 labeled with AuNPs) and capture DNA probes. The excess DNA strands could be removed by washing, which reduced the background effectively.

Simulated dsDNA in different concentrations was also determined by the proposed method. The calibration curve of Figure 6(b) shows a good correlation between the ^{197}Au signal and the logarithm of the concentration of the target dsDNA (correlation coefficient of r^2=0.9659) in the range from 10^2 pM to 10^4 pM. The precision for the concentration of the target DNA at 10^3 pM with three replicate measurements was 5.5% (RSD). The detection limit (LOD, 3σ) was about 39.17 pM.

Comparing the LODs of Various DNA Hybridization Assays

The sensitivity could be enhanced using AuNP tags instead of metal ions for the nanoparticles containing numerous metal atoms (28). Moreover, streptavidin has four binding sites for biotin, making it possible to couple more tags per streptavidin molecule which can further increase the sensitivity of the assay. The LOD of the developed method for the synthesized 28-base ssDNA target was compared with some values derived from the literature (6, 18, 19, 31) for direct DNA hybridization assays with AuNPs tags. As shown in Table III, the LOD obtained by the present method is better than those of others.

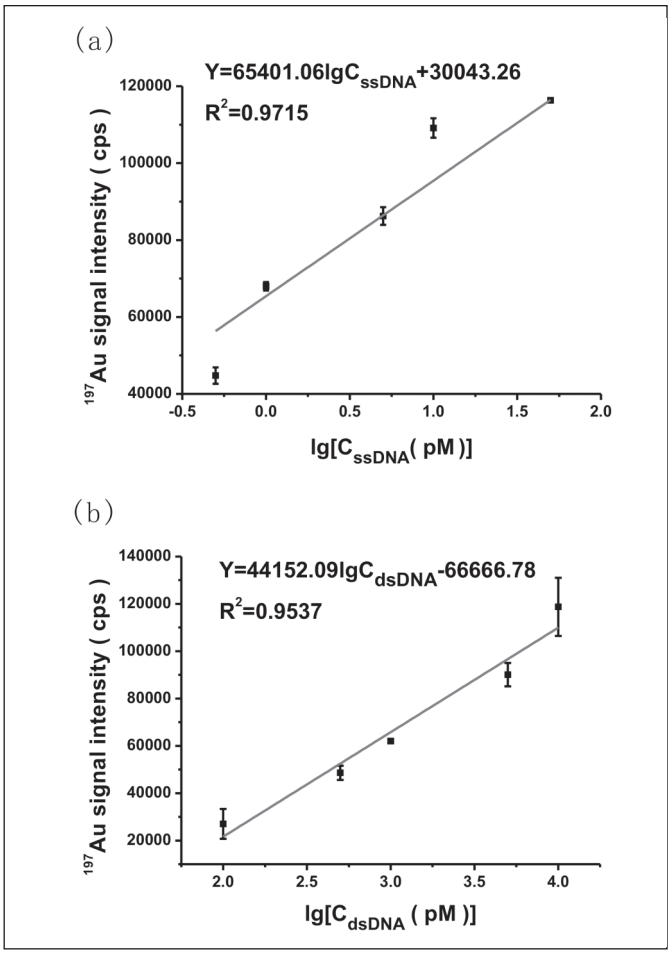

Fig. 6 (a and b). Correlation between the ^{197}Au signal intensity and the logarithm of (a) target ssDNA (the concentration varied from 0.5 to 50 pM) and (b) simulated dsDNA (the concentration varied from 10^2 to 10^4 pM). 100 ng g^{-1} ^{103}Rh was spiked into the solution as an internal standard.

TABLE III
Comparison of Various DNA Assays Based on the AuNPs Labels

Detection Methods	Dynamic Range	LOD	References
Colorimetry	0.25–50 nM	50 pM	(31)
ICP-MS	1–100 pM	1 pM	(18)
ICP-AES	350–3.5×10^6 pM	350 pM	(19)
ETV-AAS	10–200 pM	3 pM	(6)
ICP-MS	0.5–50 pM	0.39 pM	This work

CONCLUSION

A valid method based on a DNA hybridization assay and AuNPs labeling for the accurate ICP-MS determination of specific target DNA related to *Shigella flexneri* was studied. Highly efficient hybridization was verified by the signal intensity from the hybridized complexes. The convenient separation process for hybridized complexes was accomplished by the effective and low-cost system of biotin-streptavidin affinity. This study indicates that ICP-MS coupled with a DNA hybridization assay is a promising method for the sensitive detection of specific DNA of *Shigella flexneri* and provides new insights into the quantification of low abundance nucleic acids in biological samples without amplification of PCR. It has great potential for the determination of various bacterial pathogens by ICP-MS-based multiplex assay with multiplex NP tags using oligonucleotide hybridization strategy in the future.

ACKNOWLEDGMENT

This work was supported by the China Scholarship Council, the National Nature Science Foundation of China (No. 41521001 and No. 21207120), the Ministry of Science and Technology of China (No. 2014DFA20720), and the Research Program of the State Key Laboratory of Biogeology and Environmental Geology of China.

Received March 20, 2017.

REFERENCES

1 J. Shendure, and H.L. Ji, Nat. Biotechnol. 26, 1135 (2008).

2 D.J. Lockhart, H.L. Dong, M.C. Byrne, M.T. Follettie, M.V. Gallo, M.S. Chee, M. Mittmann, C.W. Wang, M. Kobayashi, H. Horton, and E.L. Brown, Nat. Biotechnol. 14, 1675 (1996).

3 M.A. Nadkarni, F.E. Martin, N.A. Jacques, and N. Hunter, Microbiology-(UK) 148, 257 (2002).

4 M.J. Espy, J.R. Uhl, L.M. Sloan, S.P. Buckwalter, M.F. Jones, E.A. Vetter, J.D.C. Yao, N.L. Wengenack, J.E. Rosenblatt, F.R. Cockerill, and T.F. Smith, Clin. Microbiol. Rev. 19, 165 (2006).

5 L. Gutierrez, M. Mauriat, J. Pelloux, C. Bellini, and O.V. Wuytswinkel, Plant Cell 20, 1734 (2008).

6 X.M. Xu, Y. Gao, S.X. Zhang, S.Z. Li, T. Bai, Y. Zhang, X.R. Hu, and R. Liu, Microchem J. 126, 302 (2016).

7 L. Chen, Y. Wang, D.F. Cheng, X.R. Liu, S.P. Dou, G.Z. Liu, D.J. Hnatowich, and M. Rusckowski, Bioorg. Med. Chem. 21, 6523 (2013).

8 M.K. Dewanjee, A.K. Ghafouripour, R.K. Werner, A.N. Serafini, and G.N. Sfakianakis, Bioconj. Chem. 2, 195 (1991).

9 H.A. Bassler, S.J.A. Flood, K.J. Livak, J. Marmaro, R. Knorr, and C.A. Batt, Appl. Environ. Microbiol. 61, 3724 (1995).

10 E. Avanissaghajani, K. Jones, D. Chapman, and C. Brunk, Biotechniques 17, 144 (1994).

11 J. Kwun, S. Yun, L. Park, and J.H. Lee, Talanta 119, 262 (2014).

12 G. Han, S. Zhang, Z. Xing, and X. Zhang, Angew. Chem. Int. Ed. 52, 1466 (2013).

13 Y.C. Luo, X.W. Yan, Y.S. Huang, R.B. Wen, Z.X. Li, L.M. Yang, C.J. Yang, and Q.Q. Wang, Anal. Chem. 85, 9428 (2013).

14 F. Li, Q. Zhao, C.A. Wang, X.F. Lu, X.F. Li, and X.C. Le, Anal. Chem. 82, 3399 (2010).

15 R. Liu, P. Wu, L. Yang, X.D. Hou, and Y. Lv, Mass Spectrom. Rev. 33, 373 (2014).

16 S. Hu, R. Liu, S. Zhang, Z. Huang, Z. Xing, and X. Zhang, J. Am. Soc. Mass. Spectrom. 20, 1096 (2009).

17 G. Han, Z. Xing, Y. Dong, S. Zhang, and X. Zhang, Angew. Chem. Int. Ed. 50, 3462 (2011).

18 S.X. Zhang, G.J. Han, Z. Xing, S.C. Zhang, and X.R. Zhang, Anal. Chem. 86, 3541 (2014).

19 L.L. Wu, L.W. Qiu, C.S. Shi, and J. Zhu, Biomacromolecules 8, 2795 (2007).

20 K.L. Kotloff, J.P. Winickoff, B. Ivanoff, J.D. Clemens, D.L. Swerdlow, P.J. Sansonetti, G. Adak, and M. Levine, Bull. W.H.O. 77, 651 (1999).

21 D.M. Deer, and K.A. Lampel, J. Food Prot. 73, 1618 (2010).

22 M.J. Hosseini, and A.R. Kaffashian, Arch. Iran. Med. 13, 413 (2010).

23 G. Frens, Nature Phys. Sc.i 241, 20 (1973).

24 C.C. Huang, Y.F. Huang, Z.H. Cao, W.H. Tan, and H.T. Chang, Anal. Chem. 77, 5735 (2005).

25 R. Elghanian, J.J. Storhoff, R.C. Mucic, R.L. Letsinger, and C.A. Mirkin, Science 277, 1078 (1997).

26 J. Thavanathan, N.M. Huang, and K.L. Thong, Biosensors & Bioelectronics 55, 91 (2014).

27 K. Brueckner, K. Schwarz, S. Beck, and M.W. Linscheid, Anal. Chem. 86, 585 (2014).

28 Q. He, Z.L. Zhu, L.L. Jin, L. Peng, W. Guo, and S.H. Hu, J. Anal. At. Spectrom. 29, 1477 (2014).

29 P.J. Ginel, J.M. Margarito, J.M. Molleda, R. Lopez, and M. Novales, Res. Vet. Sci. 60, 107 (1996).

30 B.S. Li, L.F. Zhao, C. Zhang, X.H. Hei, F. Li, X.B. Li, J. Shen, Y.Y. Li, Q. Huang, and S.Q. Xu, Anal. Sci. 22, 1367 (2006).

31 X. Mao, H. Xu, Q.X. Zeng, L.W. Zeng, and G.D. Liu, Chem. Commun. 21, 3065 (2009).

Application of Supramolecular Microextraction and Flame Atomic Absorption Spectrometry for Ultra-trace Determination of Cadmium in Food and Water Samples

Z.A. ALOthman[a], M.A. Habila[a], Erkan Yilmaz[b], M. Soylak[b, *], and A.A. Alwarthan[a]
[a] Chemistry Department, College of Science, King Saud University, Riyadh 11451, Kingdom of Saudi Arabia
[b] Erciyes University, Faculty of Sciences, Department of Chemistry, 38039 Kayseri, Turkey

ABSTRACT

In this work, a supramolecular microextraction procedure for trace cadmium as 1,2,4 thiadiazole-2,5 dithiol chelates has been established. Flame atomic absorption spectrometry was used for the determination of cadmium. A rapid injection of 600 µL tetrahydrofuran and 200 µL of 1-decanol in a sample solution containing cadmium at pH 8 leads to formation of a cloudy solution by ultrasonic waves. Then the supramolecular organic solvent mixture, including the chelated cadmium, was separated by centrifugation. Certified reference materials (TMDA 64.2 and TMDA 53.3) were tested and the determined concentrations were in agreement with the certified values. Furthermore, the method resulted in an LOD of 0.46 µg L^{-1}, LOQ of 1.37 µg L^{-1}, and RSD of 5.1%. The supramolecular microextraction procedure was successfully applied for the analysis of environmental samples including wastewater, seawater, dam water, valley water, and black pepper.

INTRODUCTION

Metal ions at trace or ultratrace levels are generally problematic for humans, plants, and animals (1-3). Lead (Pb) and cadmium (Cd) are very toxict metals even at trace levels, whereas zinc (Zn) and copper (Cu) are toxic only when they are present at higher concentrations (4-7). Excessive use of fertilizers can accumulate trace elements in the soil, causing high toxicity to the environment and plants. Cadmium contamination in the food chain can be harmful and cause chronic health problems (8-13).

The determination of cadmium and other metals at trace or ultratrace levels by spectroscopic techniques are an important area of chemistry, agriculture, medicine, biology, etc. (14-20). Due to the low detection capabilities of these techniques, the matrix effects and low levels of the analyte elements in some samples are two important problems (21-25). Preconcentration-separation systems, including solid phase extraction, cloud point extraction, coprecipitation, membrane filtration, electrodeposition and flotation, are an important key to solve these problems (26-29).

In the last decade, microextraction techniques have become an alternative for the preconcentration-separation techniques due to advantages such as limited consumption of organic solvents, the possibility of high preconcentration factors, and easy application to real samples, etc. (30-33). The use of suitable new solvents in microextraction studies which are environmentally friendly and green is a challenge that has been discussed by analytical chemists (34-36). Supramolecular solvents (SUPRAS) for microextraction are a good choice (36-38). SUPRAS has been introduced as an extraction method with many advantages such as low use of organic solvents, high pre-concentration factors, and fast and simple procedure based on a self-assembly process of the supramolecular solvent. This procedure allows the different polarity sites in these assembly constituents and provides a suitable environ-ment to separate and preconcentrate the analytes (36-38).

A novel and simple supramolecular microextraction procedure based on the extraction of Cd(II) as 1,2,4-thiadiazole-2,5-dithiol chelates is presented in this work. The analytical conditions for quantitative extraction of Cd(II) were optimized.

EXPERIMENTAL

Instrumentation

A PerkinElmer® Model 3110 flame atomic absorption spectrometer (PerkinElmer, Inc., Shelton, CT, USA) with an air–acetylene flame and hollow cathode lamp was used to measure cadmium concentrations. The instrumental operating parameters and linear range for cadmium are listed in Table I. The instrumental parameters were adjusted as recommended by the manufacturer. The samples were injected into the AAS with a Teflon® funnel using a homemade micro-sample introduction system. The absorbance signal was measured according to peak height in the continuous aspiration mode (39).

A Nel pH-900 (Ankara, Turkey) and Metrohm pH meter (Model 691, Switzerland) with a combined glass electrode were used for the pH measurements. An ALC PK 120 Model centrifuge (Buckinghamshire, England) was used for centrifugation. A vortex mixer (VWR International LLC, USA) and an ultrasonic bath (Sonorex, Model No. DT-255, Bandelin Co., Germany) were used.

**Corresponding author.*
:E-mai: soylak@erciyes.edu.tr
Fax: +903524374933

Reagents and Standard Solutions

All chemicals were of analytical grade. Distilled and deionized water with 18 MΩ resistivity were prepared using a Milli-Q® system (Millipore Corporation, USA). Stock Cd(II) solutions (1000 mg L^{-1}) were prepared by dissolving the nitrate salt in water (E. Merck. Darmstadt, Germany). Working standard solutions were obtained via serial dilution of a stock standard solution. The 0.1% (w/v) 1,2,4-thiadiazole-2,5-dithiol (Sigma-Aldrich, St. Louis, MO, USA) solution was prepared using deionized water.

Procedure

A 20-mL sample solution containing Cd(II) was placed into a 50-mL polypropelene centrifuge tube and the pH was adjusted to 8 using an ammonia buffer solution. Then 200 µL of 0.1% 1,2,4-thiadiazole-2,5-dithiol ligand was introduced. In this step, the chelation of Cd(II) with 1,2,4-thiadiazole-2,5-dithiol occurred. Then, a solution of tetrahydrofuran and 1-decanol was rapidly injected into the mixture which leads to the formation of supramolecular solvent inside the tube. The mixture was exposed to ultrasonic waves for 4 to 5 minutes and then shaken on the vortex for one minute. Finally, the phase was separated by using the centrifuge at 4000 rpm for 10 minutes. After removing the bottom aqueous phase, the remaining supramolecular solvents containing cadmium as 1,2,4-thiadiazole-2,5-dithiol chelates were dissolved in ethanol to complete the final volume to 500 µL. The Cd(II) concentration was determined by injection of 50 µL into the AAS with a Teflon® funnel using a homemade micro-sample introduction system.

Application of Method to Real Samples

Water samples, including wastewater, seawater, dam water, and valley water were obtained in Turkey. The samples were filtered with a Millipore® cellulose membrane (0.45 micrometer), then the optimized supramolecular microextraction procedure was applied for Cd(II) determination. Certified reference materials for water such as TMDA 64.2 and TMDA 53.3 (National Water Research Institute, Environment Canada, Burlington, Canada) were applied to evaluate the process. In addition, black pepper as a food sample from Kayseri City, Turkey, was collected, washed, dried, and digested as described in the literature (31, 39). The proposed supramolecular microextraction steps were applied to the food sample extract for Cd(II) determination.

RESULTS AND DISCUSSION

Optimization of Analytical Parameters

The significant parameters controlling the supramolecular extraction steps including pH, amount of 1,2,4-thiadiazole-2,5-dithiol as ligand, composition of supramolecular mixture, and sample volume, were optimized.

The pH of the sample solution containing Cd(II) was tested in acidic, neutral and basic medium up to pH 9. Figure 1 shows the effect of pH on the recovery of Cd(II). The quantitative recovery was achieved at pH 8 which was selected for further investigations. It was reported earlier that the pH of a sample solution significantly affects the recovery of heavy metals (14, 16, 18, 21).

The volume of 1,2,4-thiadiazole-2,5-dithiol as ligand was tested in the range of 0–300 µL and the (%) recovery was calculated for each case. Figure 2 demonstrates that the (%) recovery values were very low at 0, 25, and 50 µL, then increased at 100 and 150 µL. Quantitative recoveries were obtained between 200 to 300 µL. The increase in recoveries between increasing volume of ligand solution can be attributed to the fact that the microextraction procedure depends on the formation of a complex between Cd(II) and 1,2,4-thiadiazole-2,5-dithiol as the ligand. This complex will leave the aqueous phase and move to the organic supramolecular solvent phase which separates later and is measured. When using a limited amount of 1,2,4-thiadiazole-2,5-dithiol ligand, it will not be enough to chelate all Cd(II). Therefore, 200 µL was chosen for further experiments.

The component of the supramolecular solvent is reported to have significant effects on the recovery of metals (39). Therefore, tetrahydrofuran with 1-decanol, tetrahydrofuran with undecanol, and tetrahydrofuran with decanoic acid were tested as different supramolecular solvents and the recovery was 99%, 18%, 7%, respectively. Tetrahydrofuran was selected for further work due to quantitative recoveries.

The volume of tetrahydrofuran and the amount of 1-decanol were investigated in the range of 0–800 µL for tetrahydrofuran and in the range of 0–250 µL for 1-decanol. The quantitative recoveries (>95%) were obtained for 600–800 µL of tetrahydrofuran and for 200–250 µL of 1-decanol. For further work,

TABLE I
Instrumental Operating Conditions and Linear Range for Cadmium

Element	Wavelength (nm)	Slit Width (nm)	Lamp Current (mA)	Linear Range (µg mL^{-1})
Cd	228.8	0.7	4	0.1 – 2.0

600 µL of tetrahydrofuran and 200 µL of 1-decanol were selected.

The effect of sample volume is a controlling parameter which directly affects the preconcentration factor (40–46) and was studied in the range from 10 mL to 45 mL (Figure 3). The results show that the recoveries for Cd(II) were quantitative up to 20 mL. The preconcentration factor calculated as the ratio between the initial volume of the Cd(II) sample and the last volume after supramolecular microextraction was 40, considering that the last volume is 0.5 mL.

The optimum conditions for the quantitative recoveries of Cd(II) as 1,2,4-thiadiazole-2,5-dithiol chelates for the presented supramolecular extraction method are summarized in Table II.

Matrix Effects

The studies on the effect of common interfering ions on the recovery of analyte elements are important for the optimization of separation-preconcentration methods (47-54). This was tested by applying the supramolecular separation- preconcentration steps in the presence of K^+, Cl^-, Mg^{2+}, Ca^{2+}, SO_4^{2-}, F^-, Ni^{2+}, Cu^{2+}, Fe^{3+}, Zn^{2+}, CO_3^{2-}, NO_3^-, and Na^+. Table III presents the % recovery of cadmium for each ion which was not less than 96%, indicating that these supramolecular extraction steps can be applied for different samples with various matrices.

Analytical Figures of Merit

The LOD for this process was 0.46 µg L^{-1}, the LOQ was 1.37 µg L^{-1}, and the relative standard deviation (RSD) was 5.1%. The supramolecular microextraction procedure described in this work was compared with others from the literature (55–61) and showed comparable results (Table IV).

Application

Validation of the presented supramolecular microextraction

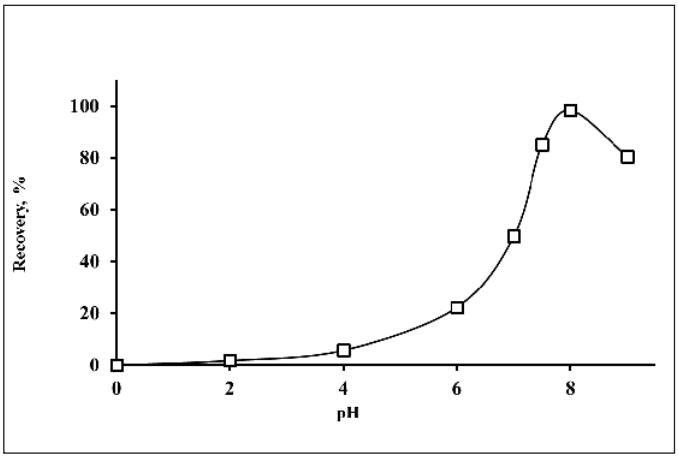

Fig 1. Evaluation of the effect of pH value on the recovery of Cd(II) (N=3).

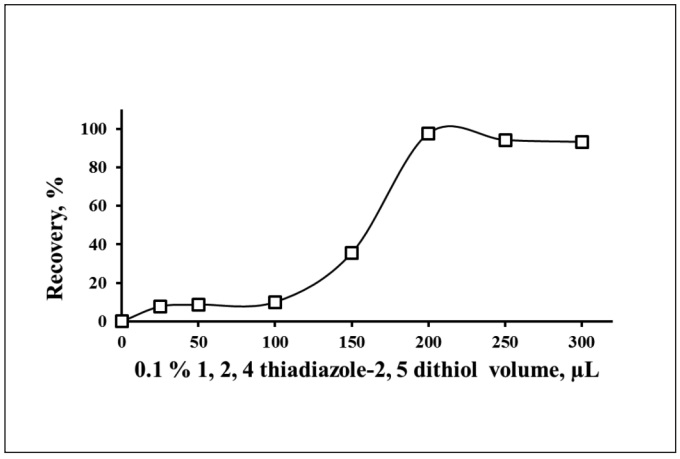

Fig. 2. Evaluation of the effect of the quantity of ligand on the (%) recovery of Cd(II) (N=3).

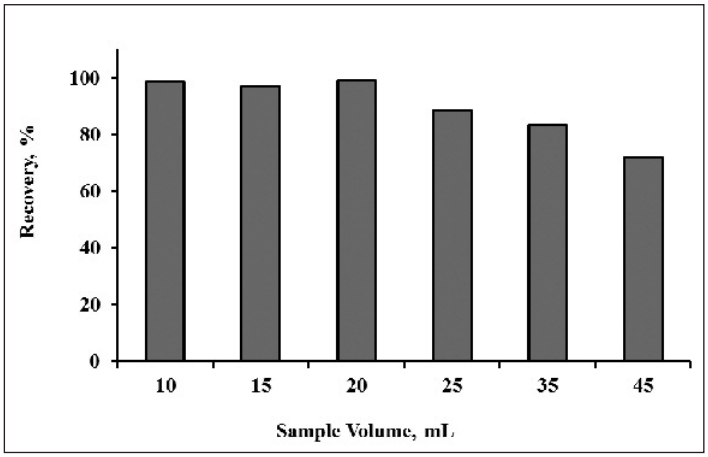

Fig. 3. Effect of sample volume on the (%) recovery of Cd(II) (N=3)

TABLE II
Optimum Condition for Cd(II) Supramolecular Microextraction

Parameters	Optimum Values
pH value of sample solution	8
Amount of 0.1% 1, 2, 4 thiadiazole-2, 5 dithiol	200 µL
Amount of tetrahydrofuran	600 µL
Amount of 1-decanol	200 µL
Sample volume	20 mL

procedure for Cd(II) was investigated by addition/recovery tests of a tap water sample from Erciyes University, Kayseri, Turkey (Table V). The procedure is applicable in the presence of different concentrations of Cd(II) where the recoveries were not less than 99%. For further optimization, certified reference materials TMDA 64.2 and TMDA 53.3 Water were applied (Table VI). The concentrations found by using the presented procedure were in agreement with the certified values.

Different samples such as wastewater, seawater, dam water, valley water, and black pepper were used for the determination of Cd(II) content. Table VII lists the obtained results which reveal that the developed procedure is applicable and independent of type of matrix.

CONCLUSION

A microextraction procedure, based on the application of tetrahydrofuran with 1-decanol to form a supramolecular solvent to separate Cd(II), was optimized. The 1,2,4-thiadiazole-2,5-dithiol as ligand plays an important role for Cd(II) separation and recovery. The maximum operating conditions were a pH of 8 and using 200 µL of 0.1% 1,2,4-thiadiazole-2,5-dithiol, 600 µL of tetrahydrofuran, and 200 µL of 1-decanol. The initial sample volumes can be increased to 20 mL to obtain quantitative recoveries. The procedure showed high efficiency compared to other methods provided in the literature.

TABLE III
Effect of Some Common Interfering Ions on the Recovery (%) of Cd(II) (N=3)

Ions	Concentration (µg mL^{-1})	Added as:	Recovery (%)
K^+, Cl^-	2000	KCl	99.5±0.5
Mg^{2+}	800	$Mg(NO_3)_2 \cdot 6H_2O$	98.5±0.3
Ca^{2+}	800	$CaCl_2$	99.5±0.4
SO_4^{2-}	500	Na_2SO_4	98.0±0.6
F^-	500	NaF	96.5±0.4
Ni^{2+}	5	$Ni(NO_3)_2 \cdot 6H_2O$	98.0±0.6
Cu^{2+}	10	$Cu(NO_3)_2 \cdot 3H_2O$	100.0±0.4
Fe^{3+}	5	$Fe(NO_3)_3 \cdot 9H_2O$	96.0±0.4
Zn^{2+}	5	$Zn(NO_3)_2$	97.0±0.8
CO_3^{2-}	2000	Na_2CO_3	97.0±0.4
NO_3^-	2000	KNO_3	99.0±0.4
Na^+	8000	NaCl	96.0±0.3

TABLE IV
Comparison Between Proposed Procedure and Other Methods Reported in the Literature for Cu Determination

Preconcentration Method	LOD (µg L^{-1})	Ref.
Dispersive liquid–liquid microextraction (DLLME)	1.0	(55)
Dispersive liquid–liquid microextraction (DLLME)	0.4	(56)
On-line solvent extraction	0.003	(57)
Cloud Point Extraction (CPE)	0.006	(58)
Cloud Point Extraction (CPE)	0.31	(59)
Microprecipitation	0.25	(60)
Supramolecular microextration (SME)	0.46	This study

TABLE V
Addition/Recovery Evaluation of Developed Procedures for Cd(II) from a Tap Water Sample from Erciyes University (N=3)

Added (µg)	Found (µg)	Recovery (%)
0	0	-
0.50	0.49±0.11	99
1.0	1.0±0.13	100

TABLE VI
Validation of Developed Microextraction Procedure Using TMDA 64.2 and TMDA 53.3 Water CRMs (N=3)

CRM	Certified Value (µg L^{-1})	Found Value (µg L^{-1})	Recovery (%)
TMDA 64.2	288	282±4	98
TMDA 53.3	118	117±5	99

TABLE VII
Application of Developed Supramolecular Microextraction Method for Cd Determination in Water and Food Samples (N=3)

Sample	Concentration
Wastewater	10.2±0. 5 µg L^{-1}
Seawater	26.5±0.4 µg L^{-1}
Dam water	3.9±0.2 µg L^{-1}
Valley water	47.9±0.4 µg L^{-1}
Black pepper	0.8±0.2 µg g^{-1}

ACKNOWLEDGMENTS

The authors extend their appreciation to the International Scientific Partnership Program ISPP at King Saud University for funding this research work through ISPP #0029.

Received July 6, 2016.

REFERENCES

1. O. Turkoglu and, M. Soylak, and I. Belenli, Collect. Czech. Chem. C. 68, 1233 (2003).
2. M. Soylak, and O. Turkoglu, J. Trace Microprobe T., 17, 209 (1999).
3. T.Y. Gorgulu, O.D. Ozdemir, A.S. Kipcak, M.B. Piskin, and E.M. Deru, Appl. Biol. Chem. 59, 425 (2016).
4. U.A. Barbosa, I.F. dos Santos, A.M.P. dos Santos, and S.L.C. Ferreira, Anal. Lett. 49, 799 (2016)
5. M. Soylak and L. Elci, J. Trace Microprobe T., 18, 397 (2000).
6. M. Gebrelibanos, N. Megersa, and A.M. Taddesse, Int. J. Food. Contam. 3, 2 (2016). DOI 10.1186/s40550-016-0025-7
7. I. Narin, M. Soylak, and L. Elci, Anal. Lett. 34, 1935 (2001).
8. V.G. Bizarro, E.J. Meurer, and F.R.P. Tatsch, Ciencia Rural 38, 247 (2008).
9. A. Tumuklu, M. Çiflikli, and F.Z. Özgür, Asian J. Chem., 20, 6376 (2008).
10. M. Kramarova, P. Massanyi, A. Jancova, R. Toman, J. Slamecka, F. Tataruch, J. Kovacik, J. Gasparik, P. Nad, M. Skalicka, B. Korenekova, R. Jurcik, J. Cubon, and P. Hascik, Bull. Vet. Inst. Pulawy 49, 465 (2005).
11. U. Divrikli, M. Soylak, L. Elci, and M. Dogan, J. Trace Microprobe T. 21, 713 (2003).
12. M.N. AlKathiri and A.F. AlAttar, Bull. Environ. Contam. Toxicol. 58, 726 (1997).
13. A.A. AlWarthan and H.M. AlSwaidan, Arab. Gulf. J. Sci. Res. J., 13, 453 (1995).
14. M. Tuzen and M. Soylak, J. Hazard. Mater. 164, 1428 (2009).
15. Y. Yang, F.S. Zhang, H.F. Li, and R.F. Jiang, J. Environ. Manage. 90, 1117 (2009).
16. D. Mendil, O.F. Unal, M. Tuzen, and M. Soylak, Food Chem. Toxicol. 48, 1383 (2010).
17. J.S. Barin, F.R. Bartz, V.L. Dressler, J.N.G. Paniz, and E.M.M. Flores, Anal. Chem. 80, 9369 (2008).
18. A. Shokrollahi, M. Ghaedi, O. Hossaini, N. Khanjari, M. Soylak, J. Hazard. Mater. 160, 435 (2008).
19. M.A. Zazouli, M. Shorkzadeh, S. Fathi, and H. Izanlo, Afr. J. Biotechnol. 7, 3689 (2008).
20. P. Nad, P. Massanyi, M. Skalicka, B. Korenekova, V. Cigankova, and V.Almasiova, J Environ. Sci. Heal. A 42, 2017 (2007).
21. M. Soylak, L. Elci, and M. Dogan, Anal. Lett. 26, 1997 (1993).
22. M. Karimi, A.M.H. Shabani and S. Dadfarnia, J. Braz. Chem. Soc. 27, 144 (2016).
23. M. Tuzen, M. Soylak, D. Citak, H.S. Ferreira, M.G.A. Korn, and M.A. Bezerra, J. Hazard. Mater. 162, 1041 (2009).
24. S. Kaur, T.P.S. Walia, and R.K. Mahajan, J. Environ. Eng. Sci. 7, 83 (2008).
25. A. Uzun, M. Soylak, L. Elci, and M. Dogan, Asian J. Chem., 14, 1277 (2002).
26. S. Dadfarnia, A.M. Haji Shabani, and M. Amirkavei, Turk. J. Chem., 37, 746 (2013).
27. U. Divrikli, A.A. Kartal, M. Soylak, and L. Elci, J. Hazard. Mater., 145, 459 (2007).
28. A. Denizli, E. Piskin, and B. Salih, Turk. J. Chem. 19, 296 (1995).
29. H. Cesur, Turk. J. Chem., 27, 307 (2003).
30. Y.E. Unsal, M. Tuzen, and M. Soylak, Turk. J. Chem., 38, 173 (2014).
31. Z.A. ALOthman, E. Yilmaz, M. Habila, and M. Soylak, Desalin. Water Treatmt. 51, 6770 (2013).
32. M. Amirkavei, S. Dadfarnia and A.M. Haji Shabani, Quim. Nova 36, 63 (2013).
33. R. Yousefi and F. Shemirani, Anal. Chim. Acta 669, 25 (2010).
34. C. Caballo, M.D. Sicilia, and S. Rubio, Talanta 119, 46 (2014).
35. C. Caballo, M. D. Sicilia, and S. Rubio, Anal Bioanal. Chem. 407, 4721 (2015).
36. Q. Yang, W. Su, X. Jiang, and X. Chen, Int. J. Environ. Anal. Chem. 94, 812 (2014).
37. M. Peyrovi and M. Hadjmohammadi, J. Chromatogr. 980B, 41 (2015).
38. F. Aydin, E. Yilmaz, and M. Soylak, RSC Adv. 5, 40422 (2015).
39. E. Yilmaz and M. Soylak, Talanta 126, 191 (2014).
40. S. Saracoglu, M. Soylak, D.S.K Peker, L. Elci, W.N.L. dos Santos, V.A. Lemos, and S.L.C. Ferreira, Anal. Chim. Acta 575, 133 (2006).
41. M. Soylak, Y.E. Unsal, N. Kizil, and A. Aydin, Food Chem. Toxicol., 48, 517 (2010).
42. M. Ghaedi, M. Montazerozohori, F. Marahel, M.N. Biyareh, and M. Soylak, Chin. J. Chem. 29, 2141 (2011).
43. I.M.M. Kenawy, W.I. Mortada, Y.G. Abou El-Reash, and A.H. Hawwas, Can. J. Chem. 94, 221 (2016).
44. M. Soylak and E. Yilmaz, Desalination 275, 297 (2011).
45. L. Hu, Y. Cai, and G. Jiang, Chemosphere 156, 14 (2016).
46. M. Sheibani, F. Marahel, M. Ghaedi, M. Montazerozohori, and M. Soylak, Toxicol. Environ. Chem. 93, 860 (2011).
47. M. Soleimani and Z.H. Siahpoosh, J. Applied Chem. Research 9, 7 (2015).
48. M. Ghaedi, K. Niknam, E. Niknam, K. Mortazavi, K. Taheri, and M. Soylak, J. Chin. Chem. Soc. 57, 275 (2010).
49. M. Firlak, S. Cubuk, E.K. Yetimoğlu, and M.V. Kahraman, Chem. Pap. 70, 757 (2016).
50. H. Erdogan, O. Yalcinkaya, and A.R. Turker, Turk. J. Chem., 40, 772 (2016). 51. N. Khan, T.G. Kazi, M. Tuzen, and M. Soylak, Desalin.

Water Treatmt. 55, 1088 (2015).

52. C. Polat, V. Eyupoglu, and O.N. Sara, AIP Conf. Proc. 1726, 020110 (2016); DOIi: 10.1063/1.4945936

53. R. Gurkan and M. Eser, J. Iran. Chem. Soc. 13, 1579 (2016).

54. X. Xu, M. Zhang, L. Wang, S. Zhang, M. Liu, N. Long, X. Qi, Z. Cui, L. Zhang, Food Anal. Methods 9, 1696 (2016).

55. A. Afkhami, T. Madrakian, H. Siampour, J. Hazard. Mater. 138, 269 (2006).

56. S.Z. Mohammadi, Y.M. Baghelani, F. Mansori, T. Shamspur, D. Afzali. Quim. Nova 35, 198 (2012).

57. A.N. Anthemidis, G.A. Zachariadis, and J.A. Stratis, J. Anal. At. Spectrom. 18, 1400 (2003).

58. X. Zhu, X. Zhu, and B. Wang, Microchim. Acta 154, 95 (2006).

59. J.L. Manzoori and G. K. Nezhad, Anal. Chim. Acta 521, 173 (2004).

60. Z.A. ALOthman, M.A. Habila, S.M. Alfadul, E. Yilmaz and M. Soylak. Anal. Methods 8, 3545 (2016).

61. M. Soylak, S. Saracoglu, L. Elci, and M. Dogan, Int. J. Environ. Anal. Chem. 82, 225 (2002).

Magnetic Solid Phase Extraction of Trace Lead and Copper on Chromotrope FB Impregnated Magnetic Multiwalled Carbon Nanotubes From Cigarette and Hair Samples for Measurement by Flame AAS

Mustafa Soylak* and Zeliha Erbas
Erciyes University, Faculty of Sciences, Department of Chemistry, 38039 Kayseri, Turkey

ABSTRACT

A novel and simple magnetic-solid phase extraction procedure for the separation-preconcentration of lead(II) and copper(II) at trace levels has been established by using Chromotrope FB impregnated magnetic multiwalled carbon nanotubes as a new adsorbent. The influences of critical analytical parameters like pH, flow rates, eluent, and sample volume were optimized. Matrix effects were also examined. Analyte elements were quantitatively recovered at pH 6.0. The limit of detection values were 11.7 μg L^{-1} for lead and 3.7 μg L^{-1} for copper. The (%) RSD values were generally found at < 7%. The validation was performed by the analysis of NCS-DC73349 Bush Branches and Leaves certified reference material. The method was applied to the FAAS determination of lead and copper concentrations in cigarette and hair samples.

INTRODUCTION

The levels of trace elements are an important component of safety and quality of the environment. Trace elements such as lead (Pb), arsenic (As), and cadmium (Cd) are generally recognized as pollutants and are harmful to the health of humans, plants, and animals (1-4). They are toxic when present in excessive amounts (5-8). Metals occur naturally in soil, plants, and air. However, their concentrations are usually increased due to anthropogenic activities such as from industry and traffic (9-12).

Lead is one of the toxic elements even at ultra-trace levels (13, 14) and is absorbed in humans through inhalation of air, dermal exposure, and ingestion of dust and soil. Other sources of lead are polluted water and lead-adulterated foods (15-18). Copper (Cu) is another critical, important and necessary trace element for humans, plants, and animals. It is an essential part of several enzymes, essential for human nutrition (19-20), and necessary for the synthesis of hemoglobin (21-23). Consequently, an analytical method to preconcentrate, separate, and determine trace elements in environmental samples including natural waters is very important.

Classical solvent extraction, micellar extraction, flotation, coprecipitation and membrane filtration are popular separation-preconcentration methods for trace elements from environmental and food samples (24-28). Solid phase extraction is a popular separation-enrichment technique using novel nanomaterials with a high adsorption capacity and high surface area with resistivity to concentrated acids and bases (29-31).

In the present work, Chromotrope FB impregnated magnetic multiwalled carbon nanotubes have been used for the preconcentration -separation of Pb(II) and Cu(II) in hair and cigarette samples.

EXPERIMENTAL

Instrumentation

For this study, a Model 3110 flame atomic absorption spectrometer (PerkinElmer, Inc., Shelton, CT, USA) was used, equipped with air/acetylene flame with a 10 cm long slot burner head and hollow cathode lamps of Cu and Pb. The the conditions for flame atomic absorption spectrometty (FAAS) are given in Table I. The calibration curve equations for Cu and Pb for FAAS determinations, respectively, were (A = 0.0394 C (Cu) + 0.0056) and (A = 0.0133 C (Pb) + 0.0011), where A is the absorbance and C is the concentration of the analyte. The correlation coefficients of the equations were 0.9992 and 0.99945 for Cu and Pb, respectively.

The pH values were measured using a Sartorius PT–10 pH meter (Sartorius, Germany) with a glass electrode. A neodymium magnet was used for the phase separations. A vortex mixer (Wiggen Hauser, Malaysia) was used for thoroughly vortexing and mixing of the solutions.

Solutions and Reagents

Solutions were prepared with reverse osmosis purified water using a Milli-Q® system 18 MΩ–cm resistivity (Millipore Corporation, USA). All chemicals were of reagent grade. Stock solutions of the analyte elements were prepared from their nitrates as 1000 μg L^{-1}, solutions in 0.02 M HNO_3. Multi-walled carbon nanotubes (MWNT) (Sigma no: 636614-2G) were purchased from Aldrich, Milwaukee, WI, USA. A solution of Chromotrope FB (% 0.1 m/v) was prepared by dissolving of Chromo-trope FB No. B22328 (Alfa Aesar, Germany) in small amounts of ethanol and diluting to 50 mL with water. Certified reference material (CRM) NCS-DC73349 Bush

*Corresponding author.
e-mail: soylak@erciyes.edu.tr and msoylak@gmail.com
Tel. & Fax: +90 352 4374933

TABLE I
FAAS Instrumental Parameters

Element	Wavelength (nm)	Slit Width (nm)	Lamp Current (mA)	Flame Conditions* (a)	(b)
Cu	324.8	0.7	15	9.5	2.3
Pb	283.3	0.7	15	9.5	2.3

* (a) Air (L/min), (b) Acetylene (L/min).

Branches and Leaves (National Research Centre for Certified Reference Materials, Beijing, P.R. China) were used in the experiments for validation of the procedure.

Phosphate buffer solution (0.1 mol L^{-1}) (pH 2.0–7.0), ammonia buffer solution (0.1 mol L^{-1}) (pH 8.0), and phosphate buffer solution (0.1 mol L^{-1}) (pH 9.0) were used in the experiments.

Preparation of Chromotrope FB Impregnated Magnetic Multiwalled Carbon Nanotubes

Magnetic multiwalled carbon nanotubes were obtained according to the procedure given in the literature (32) by using magnetite. To impregnate the Chromotrope FB to the surface of the magnetic multiwalled carbon nanotubes, 1.0 g magnetic multiwalled carbon nanotubes was added to 2 mL of Chromotrope FB solution and diluted to 30 mL with reverse osmosis water and stirring continuously for 20 minutes. Afterwards, the Chromotrope FB/magnetic multiwalled carbon nanotubes were filtered off, washed with reverse osmosis water, and dried overnight at 100 °C. The amount of Chromotrope FB deposited on the magnetic multiwalled carbon nanotubes was estimated by UV-Vis spectrophotometry from the residual amount of a Chromotrope FB in the solution. It was found that 66% of Chromotrope FB was retained on the adsorbent.

Test Procedure

A 10-mL aqueous sample solution containing Pb(II) and Cu(II) was adjusted to pH 6.0 using 2 mL phosphate buffer solution. Then, 75 mg of Chromotrope FB impregnated magnetic multiwalled carbon nanotubes were added to this solution. After 5 minutes, it was vortexed with a revolution speed of 4000 rpm. After completion of the adsorption of the analytes onto the Chromotrope FB impregnated magnetic multiwalled carbon nanotubes, the adsorbent was separated at the bottom of the tube by using a neodymium magnet. The liquid phase was decanted. Then, 2 mL of 3.0 M HNO_3 in 10% acetone was added to the adsorbent for desorption of the analyte ions. Then the Chromotrope FB impregnated magnetic multiwalled carbon nanotubes were separated from the sample by using a neodymium magnet. An amount of 100 µL was aspirated into the nebulizer of the FAAS for absorbance measurements using the microinjection system.

Analysis of CRM and Real Samples

The method was also applied to CRM NCS DC73349 Bush Branches and Leaves, and cigarette and hair samples. A wet ash procedure was used for this purpose. One gram of a sample was transferred into a beaker and digested with 10 mL concentrated HNO_3 for 15 minutes at room temperature, then placed on a hot plate at 95 °C until a dry residue was obtained. The residue of each beaker was again digested with a mixture of HNO_3-H_2O_2 (2:1 v/v) until dryness. The residues in the beakers were then dissolved in 15 mL distilled water and filtered with a Whatman blue band filter paper. Then the procedure given in the "Test Procedure" was applied to these samples.

RESULTS AND DISCUSSION

Optimization

The pH is an important factor affecting quantitative adsorption of the analytes in the extraction studies (33-38). The effects of the pH on the recoveries of Pb(II) and Cu(II) ions on the Chromotrope FB impregnated magnetic multiwalled carbon nanotubes were tested at the pH range of 2.0–9.0. The results are depicted in Figure 1. The recoveries of Pb(II) and Cu(II) were found to be quantitative in the pH range of 3.0–8.0 and 5.0–7.0, respectively. For all further work, pH 6.0 was selected as optimal. The pH adjustments for pH 6.0 were done by using phosphate buffer solution.

The amounts of Chromotrope FB impregnated magnetic multiwalled carbon nanotubes were also tested

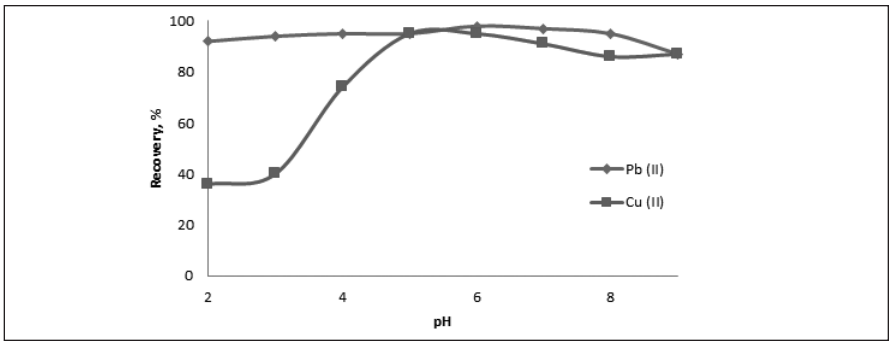

Fig. 1. Relation between pH and (%) recovery for analyte ions.

in the range of 25–100 mg. Quantitative recoveries for lead and copper ions were obtained in the range of 50–100 mg of magnetic adsorbent. An amount of 75 mg Chromotrope FB impregnated magnetic multiwalled carbon nanotubes was used for all other experiments.

The elution of the adsorbed analytes from the adsorbent is an important critical parameter (38-43). Different eluent solutions (as)listed in Table II were used to elute the adsorbed analyte elements from the Chromotrope FB impregnated magnetic multiwalled carbon nanotubes. Quantitative recoveries for both analyte ions were obtained when 2.0 mL of 3.0 M HNO_3 in 10% acetone was used as the eluent. For other elution solutions, the recovery of one analyte generally was quantitative; but the other ion was not recovered quantitatively. For all further studies, 2 mL of 3.0 M HNO_3 in 10% acetone was used as the eluent.

The volume of the samples is another key parameter for solid phase extraction studies to obtain a high preconcentration factor (44-49). The effects of the sample volume on the recoveries were examined by using 10–40 mL. The recoveries were quantitative for both Cu and Pb in the range of 10–30 mL. The recovery values were not quantitative for sample volumes higher than 30 mL. The preconcentration factor was 30 with a final volume of 2 mL.

TABLE II
Effects of Various Eluents on the Recoveries of the Analytes (Volume of Eluent: 2 mL; N=3)

Eluent Type	Recovery (%) Pb(II)	Cu(II)
0.25 M HNO_3	92±2	81±4
0.5 M HNO_3	96±3	82±4
1.0 M HNO_3	91±2	84±3
2.0 M HNO_3	94±1	88±2
3.0 M HNO_3	96±3	90±1
0.25 M HCl	87±3	86±2
0.5 M HCl	98±3	91±3
1.0 M HCl	95±4	96±3
2.0 M HCl	96±2	90±1
3.0 M HCl	94±1	91±1
0.25 N HNO_3 in 10% acetone	63±2	86±2
0.5 M HNO_3 in 10% acetone	88±1	88±1
1.0 M HNO_3 in 10% acetone	94±1	91±2
2.0 M HNO_3 in 10% acetone	95±2	94±2
3.0 M HNO_3 in 10% acetone	97±1	97±1

TABLE III
Effects of Some Matrix Ions on the Recoveries of Pb(II) and Cu(II) (N=3)

Ions	Added as:	Concentration (µg/mL)	Recovery (%) Pb(II)	Cu(II)
Na^+	$NaNO_3$	1000	97±0	99±1
K^+	KCl	1000	97±1	97±3
SO_4^{2-}	Na_2SO_4	2500	94±1	95±2
Fe^{3+}	$Fe(NO_3)_3 \cdot 9H_2O$	5	91±2	92±1
Zn^{2+}	$Zn(NO_3)_2 \cdot 6H_2O$	10	98±1	100±2
Mn^{2+}	$Mn(NO_3)_2 \cdot 4H_2O$	10	100±2	102±1
Cu^{2+}	$Cu(NO_3)_2 \cdot 3H_2O$	10	100±2	
Mg^{2+}	$Mg(NO_3)_2 \cdot 6H_2O$	100	102±0	102±2

Matrix Effects

The negative and/or positive effects of alkali, alkaline earth metals, and some metal ions at high concentrations in real samples are a big problem in the determination of trace metals (50–56). The influences of matrix components were investigated, and the results are listed in Table III. The model solution containing analyte elements and matrix components were prepared and then applied to the developed procedure as described in the Experimental section. The results clearly demonstrate that the interfering ions did not interfere with the recovery values of the analyte elements, and that the proposed method was fairly free from matrix components as given in Table III.

Analytical Features

The detection limits (LODs) of the present method for lead and copper, calculated based on 11 determinations of the standard deviation of the blank, were 11.7 µg L^{-1} and 3.7 µg L^{-1}, respectively. The relative standard deviation (RSD) determined from 11 analyses was below 5%.

Application to CRM Sample

The present method was applied to CRM NCS-DC73349 Bush Branches and Leaves to verify the validity of the method for copper and lead levels after the wet digestion procedure as given in the Experimental section. The results in Table IV show that the presented solid phase extraction method is in good agreement with the certified values of the certified reference material.

The correctness of the present procedure was also verified by analyzing the concentration after addition of known amounts of Cu and Pb onto a cigarette and a hair sample. The results listed in Table V for the cigarette sample and in Table

VI for the hair sample show that good agreement was obtained between the added and found analyte content using the present solid phase extraction system.

In addition, the analyte elements of Cu and Pb in cigarette samples (purchased at a local market in Kayseri, Turkey) and in hair samples (from healthy subjects living in Kayseri, Turkey) were determined by flame atomic absorption spectrometry. The results are listed in Table VII.

TABLE IV
Application of Present Method to CRM NCS-DC73349 Bush Branches and Leaves for the Determination of Pb and Cu (N=3)

	Lead	Copper
Certified value (μg/g)	47	6.6
Found (μg/g)	45.2±3.0	6.1±0.8
Recovery (%)	96	93

TABLE V
Addition–Recovery Tests for Cigarette Sample (N=3) Using Solid Phase Extraction

	Added (μg)	Found (μg)	Recovery (%)
Pb	0	1.14±0	
	4	5.2±0.3	95
	8	8.8±0.3	95
Cu	0	3.0±0.1	
	2	5.1±0.2	102
	4	7.0±1.0	98

TABLE VI
Addition-Recovery Tests for Hair Sample (N=3) Using Solid Phase Extraction

	Added (μg)	Found (μg)	Recovery (%)
Pb	0	0	
	16	15.2±2	95
	24	22.7±1	94
Cu	0	0.4±0.1	
	8	8.2±0.1	97
	12	12.2±1	98

Comparison of Proposed Procedure With Preconcentration Methods in Literature

A comparison between the figures of merit of the proposed method with other solid phase extraction methods used for the preconcentration/separation of copper and lead is given in Table VIII (55-62).

TABLE VII
Application of Present Procedure Using Flame AAS Analysis of Cigarette and Hair Samples (N=3)

Sample	Concentration (μg/g) Pb	Cu
Cigarette 2	BDL	13.2±0.3
Cigarette 3	BDL	7.7±0.1
Cigarette 1	BDL	10.2±0.4
Hair 2	BDL	14.6±1.0
Hair 3	BDL	5.8±1.0

BDL: below the detection limit.

CONCLUSION

A simple and novel procedure based on magnetic solid phase extraction of lead and copper at trace levels on Chromotrope FB impregnated magnetic multiwalled carbon nanotubes in hair and cigarette samples from Kayseri, Turkey, has been established. The advantages of the presented magnetic solid phase extraction method include time savings for adsorption and elution steps, low use of use of organic solvents, and the magnetic adsorbent can be used at least five times without loss of its adsorption properties.

Received November 8, 2016.

REFERENCES

1. X. H. Zhu, S. S. Lyu, P. P. Zhang, X. G. Chen, D. D. Wu, and Y. Ye, Environ. Earth. Sci. 75, 98 (2016). DOI 10.1007/s12665-015-5036-9
2. S. Saracoglu, U. Divrikli, M. Soylak, L. Elci, and M. Dogan, J. Trace Microprobe Techn. 21, 389 (2003).
3. G. Guleryuz, M. Arslan, B. Izgi, and S. Gucer, Z. Naturforsch. C 61, 357 (2006).
4. O. Turkoglu, S. Saracoglu, M. Soylak, and L. Elci, Trace Elem. Electroly. 21, 4 (2004).

TABLE VIII
Comparison of Proposed Method With Some Methods in the Literature

Adsorbent	PF[a]	LOD[b] (μg/L)	Ref.
Magnetic allylamine modified graphene oxide-poly(vinyl acetate-co-divinylbenzene) nanocomposite	40	Pb: 2.39, Cu: 2.34	32
Fe_3O_4/graphene magnetic nanoparticles	-	Pb: 0.87, Cu: 0.22	42
Core–Shell magnetic chitosan biopolymer	25	-	52
Oxidized single-walled carbon nanotubes	50	Pb:5.4, Cu: 3.9	57
Multiwalled carbon nanotubes	50	Pb:5.5, Cu:2.3	58
Chromotrope FB impregnated magnetic multiwalled carbon nanotubes	15	Pb: 11.7, Cu: 3.7	This work

[a] PF: Preconcentration factor. [b] LOD: Limit of detection.

5. D.R. Chettle, J. Radioanal. Nucl. Ch. 268, 653 (2006).
6. D. Mendil, O.F. Unal, M. Tuzen, and M. Soylak, Food Chem. Toxicol. 48, 1383 (2010).
7. E. Chirila, S. Dobrinas, and V. Coatu, Rev. Chim-Bucharest. 55, 381 (2004).
8. N. Alkan, A. Alkan, K. Gedik, and A. Fisher, Toxicol. Ind. Health 32, 447 (2016).
9. S. Savasci, and M. Akcay, Turk. J. Chem. 20, 146 (1996).
10. F. Sipahi, and S. Uslu, Arab. J. Geosci. 9, 600 (2016). DOI 10.1007/s12517-016-2620-6
11. R. Mehra, and M. Juneja, J. Ind. Chem. Soc. 81, 349 (2004).
12. N. Shaheen, N. Md. Irfan, I. N. Khan, S. Islam, Md. S. Islam, and Md.K. Ahmed, Chemosphere 152, 431 (2016).
13. F. Yalcin, S. Kilic, D. G. Nyamsari, M. G. Yalcin, and M. Kilic, Pol. J. Environ. Stud. 25, 471 (2016).
14. U. Divrikli, A. A. Kartal, M. Soylak, and L. Elci, J. Hazard. Mater. 145, 459 (2007).
15. D. S. Herman, M. Geraldine, C. C. Scott, and T. Venkatesh, Toxicol. Ind. Health 22, 249 (2006).
16. L. Vilizzi, and A.S. Tarkan, Environ. Monit. Assess. 188, 243 (2016). DOI 10.1007/s10661-016-5248-9
17. A. X. Wang, L. P. Guo, and D. M. Wu, Spectrosc. Spect. Anal. 26, 1345 (2006).
18 M. Tuzen, S. Saracoglu, and M. Soylak, J. Food Nutr. Res. 47, 120 (2008).
19. J. Semancikova, and D. Remeteiova, Holist. Approach Environ. 6, 55 (2016).
20. M. Tuzen, M. Soylak, D. Citak, H.S. Ferreira, M.G.A. Korn, and M.A. Bezerra, J. Hazard. Mater. 162, 1041 (2009).
21. M. Stanek, W. Andrzejewski, J. Mazurkiewicz, B. Janicki, D. Cygan-Szczegielniak, A. Roślewska, K. Stasiak, and I. Waszak, Pol. J. Environ. Stud. 25, 301 (2016).
22. M. Ghaedi, R. Shabani, M. Montazerozohori, A. Shokrollahi, A. Sahraiean, H. Hossainian, and M. Soylak, Environ. Monit. Assess. 174, 171 (2011).
23. E. Pip, Environ. Health Persp. 108, 863 (2000).
24. M. Tuzen, and M. Soylak, J. Hazard. Mater. 162, 724 (2009).
25. T. Stafilov, G. Pavlovska, and K. Cundeva, Turk. J. Chem. 24, 303 (2000).
26. A. Shokrollahi, M. Ghaedi, O. Hossaini, N. Khanjari, and M. Soylak, J. Hazard. Mater. 160, 435 (2008).
27. N. Ashouri, A. Mohammadi, R. Hajiaghaee, M. Shekarchi, and M.R. Khoshayan, Desalin. Water Treat. 57, 14280 (2016).
28. S. Saracoglu, M. Soylak, D. Cabuk, Z. Topalak, and Y. Karagozlu, J. AOAC Int. 95, 892 (2012).
29. C.Q. Tu, and X.R. Wen, J. Chinese Chem. Soc. 57, 356 (2010).
30. S.G. Ozcan, N. Satiroglu, and M. Soylak, Food Chem. Toxicol. 48, 2401 (2010).
31. F. Raoufi, S. Bagheri, P. Nasehi, E. Niknam, K. Niknam, and H.R. Farmani, Orient. J. Chem. 32, 575 (2016).
32. M. Khan, E. Yilmaz, B. Sevinc, E. Sahmetlioglu, J. Shah, M.R. Jan, and M. Soylak, Talanta 146, 130 (2016).
33. E. Aliyari, M. Alvand, and F. Shemirani, RSC Adv. 6, 64193 (2016).
34. R. Gao, and Z. Fan, At. Spectrosc. 37, 195 (2016).
35. X. Lopez, and V.M. Castano, J. Nanosci. Nanotechn. 8, 5733 (2008).
36. M. Soylak, L. Elci, and M. Dogan, Anal. Lett. 26, 1997 (1993).
37. E. Ghorbani-Kalhor, Microchim. Acta 183, 2639 (2016).
38. H.M. Marwani, A.E. Alsafrani, H.A. Al-Turaif, A.M. Asiri, and S.B. Khan, Bull. Mater. Sci. 39, 1011 (2016).
39. M. Soylak, Y.E. Unsal, N. Kizil, and A. Aydin, Food. Chem. Toxicol. 48, 517 (2010).
40. S.Z. Mohammadi, and A. Seyedi, Toxicol. Environ. Chem. 98, 705 (2016).
41. F.A. Aydin, and M. Soylak, J. Hazard. Mater. 173, 669 (2010).
42. Q. Yin, Y. Zhu, S. Ju, W. Liao, and Y. Yang, Res. Chem. Intermed. 42, 4985 (2016).
43. J.P.R. da Silva, G.F.B. Cruz, R.J. Cassella, and W.F. Pacheco, Quim. Nova, 39, 561 (2016).
44. M. Soylak, Anal. Lett. 37, 1203 (2004).
45. M. Roushani, Y.M. Baghelani, S. Abbasi, S.Z. Mohammadi, M. Zahedifar, and M. Mavaei, Commun. Soil. Sci. Plan. Anal. 47, 1207 (2016).
46. C. Duran, V.N. Bulut, D. Ozdes, A. Gundogdu, and M. Soylak, J. AOAC Int. 92, 257 (2009).
47. N. Khorshidi, and A. Niazi, Separ. Sci. Technol. 51, 1675 (2016).
48. M. Soylak, Fresen. Environ. Bull. 7, 383 (1998).
49. M. Khajeh, F. Saravani, M. Ghaffari-Moghaddam, and M. Bohlooli, Int. J. Vegetable Sci. 22, 266 (2016).
50. C. Maiti, R. Banerjee, and S. Maiti, D. Dhara, Des. Monomers. Polym. 19, 669 (2016).
51. B. Bitirmis, D. Trak, Y. Arslan, and E. Kenduzler, Anal. Sci. 32, 667 (2016).
52. M.H. Beyki, S. Miri, F. Shemirani, M. Bayat, and P.R. Ranjbar, Clean- Soil Air Soil Water 44, 710 (2016).
53. Z.A. AL Othman, E. Yilmaz, M. Habila, and M. Soylak, Desalin. Water Treat. 51, 6770 (2013).
54. S. Procházková, and R. Halko, Anal. Lett. 49, 1656 (2016).
55. M.H. Beyki, S. Miri, F. Shemirani, M. Bayat, and P.R. Ranjbar, Clean- Soil Air Soil Water 44, 710 (2016).
56. M. Soylak, and N. Kizil, At. Spectrosc. 34, 216 (2013).
57. S. Chen, C. Liu, M. Yang, D. Lu, L. Zhu, and Z. Wang, J. Hazard. Mater. 170, 247 (2009).
58. E. Yilmaz, and M. Soylak, Environ. Monit. Assess. 186, 5461 (2014).
59. M. Soylak, I. Narin, L. Elci, and M. Dogan, Kuwait J. Sci. Eng. 28, 361 (2001).
60. M. Soylak, and E. Yilmaz, Desalination 275, 297 (2011).
61. S. Saracoglu, M. Soylak, and L. Elci, Trace Elem. Electroly. 18, 129 (2001).
62. M. Ghaedi, M. Montazerozohori, F. Marahel, M.N. Biyareh, and M. Soylak, Chinese J. Chem. 29, 2141 (2011).

Determination of Cobalt, Iron, and Nickel in High-Purity Silicon by High-Resolution Continuum Source Graphite Furnace Atomic Absorption Spectrometry Employing Solid Sample Analysis

Marcos André Bechlin[a], Ariane Isis Barros[a], Diego Victor Babos[a], Edilene Cristina Ferreira[a], and José Anchieta Gomes Neto[a],*

[a] UNESP – Univ. Estadual Paulista, Analytical Chemistry Department
Rua Prof. Francisco Degni, 55, Quitandinha, 14800-060, Araraquara - SP, Brazil

ABSTRACT

This paper describes the development of analytical methods for the determination of cobalt, iron, and nickel in pure silicon for photovoltaic and electronics applications based on solid sampling (SS) coupled to a high-resolution continuum source graphite furnace atomic absorption spectrometer (HR-CS GFAAS). Samples were also analyzed by line-source flame atomic absorption spectrometry (LS FAAS) as a comparative technique after acid microwave-assisted digestion. Cobalt, Fe, and Ni were determined in samples of solar-grade silicon (SoG-Si) and electronic-grade silicon (EG-Si) by SS HR-CS GFAAS and LS FAAS. A paired *t*-test at a 95% confidence level showed that the SS HR-CS GFAAS methods achieve similar results to those obtained by LS FAAS. The relative standard deviations (n=12) for a sample containing 7.80 mg kg^{-1} Co, 36.2 mg kg^{-1} Fe, and 228.5 mg kg^{-1} Ni were 6.4% for Co, 6.1% for Fe, and 1.0% for Ni for SS HR-CS GFAAS. For the SS HR-CS GFAAS, the limits of detection were 0.39 mg kg^{-1} Co, 1.14 mg kg^{-1} Fe, and 5.71 mg kg^{-1} Ni. Accuracy was also checked by the analysis of high-purity silica spiked with Co, Fe, and Ni, and the recoveries were at 94.3–97.1% (Co), 86.7–109% (Fe), and 88.4–98.9% (Ni).

INTRODUCTION

Renewable energy and energy efficiency may be considered the pillars of sustainable energy, and they are now entering global markets as a result of research and development (1,2). The production of pure silicon used as a raw material by the solar photovoltaic and microelectronic industries has increased in order to supply the rapid-growth markets (3). The presence of impurities in solar-grade silicon (SoG-Si) and electronic-grade silicon (EG-Si) may significantly reduce the efficiency of semiconductor devices, solar cells, integrated circuits, etc. (4). Depending on the concentration of Co, Ni, Cr, and Fe, these elements may generate recombination centers, which will consume electrons produced by the photovoltaic effect in solar cells (5, 6). These devices may have their efficiency reduced by about 50% due to the presence of these elements (4). Thus, rigid quality control of the SoG-Si and EG-Si materials is very important.

Among the main spectroscopic techniques employed for elemental determinations, most use conventional sample introduction systems for the solutions. The conversion of SoG-Si and EG-Si solid materials into solutions is usually done by wet digestions involving mixtures of hydrofluoric acid with strong acids at high temperature (7). These procedures are arduous, time-consuming, vulnerable to sample contamination and analyte losses, involve high consumption of energy, use large quantities of hazardous reagents, and generate substantial amounts of waste. These disadvantages may be avoided by using direct solid sample analysis, an environmentally friendly method operating according to the principle of green chemistry (8).

Solid sampling (SS) has been explored for the analysis of high-purity silicon by total reflection X-ray fluorescence spectroscopy (9), laser-induced breakdown spectroscopy (10), glow discharge mass spectrometry (11), neutron activation analysis (12), secondary ion mass spectrometry (13), and laser-ablation inductively coupled plasma mass spectrometry (14). These techniques are fast, sensitive and accurate, but acquisition and maintenance costs are relatively higher than other procedures such as graphite furnace atomic absorption (GFAAS).

High-resolution continuum source graphite furnace atomic absorption spectrometry coupled to solid sampling (SS HR-CS GFAAS) brought new possibilities for elemental spectrometric analyses (15) due to the ability to correct structured background using least-squares background correction (LSBC), to measure the spectral environment in high resolution, furnish higher signal-to-noise ratios than those provided by line sources, to sum the absorbance measurement around the line core, or to sum the absorbance for different lines, to extend the linear working range by measuring at alternative lines, and to integrate auto-

** Corresponding author.*
:E-mail: anchieta@iq.unesp.br
Tel: +55 16 33019611

matic solid sampler and microbalance which may reduce errors caused by manual operations (16, 17). The SS HR-CS GFAAS method is efficiently employed for the analysis of difficult samples such as polymers (18), glass (19), coal (20), automotive catalyst (21), and others. However, little attention has been given to the solid sampling method to analyze SoG-Si and EG-Si materials.

Considering the above, this work deals with the development of analytical methods for the determination of Co, Fe, and Ni contaminants in So-GSi and EG-Si.

EXPERIMENTAL

Instrumentation

Atomic absorption measurements were carried out using an Analytik Jena ContrAA 700 graphite furnace atomic absorption spectrometer (Jena, Germany), equipped with a short-arc Xenon lamp operated in "hot-spot" mode as a continuum radiation source, a high-resolution double monochromator, and a charge-coupled device (CCD) detector. Measurements were done at the 252.136 nm (Co), 305.760 nm (Ni), and 305.909 nm (Fe) lines. The lines of Ni and Fe were within the same spectral window, so they were measured simultaneously. The integrated peak absorbance (peak volume selected absorbance) was equivalent to 3 pixels (CP ± 1; CP: central pixel corresponding to the center of the line). Solid sampling graphite tubes without a dosing hole, pyrolytically coated, and transversely heated were used throughout this work. The samples were weighed directly onto solid sampling platforms using a WZ2PW microbalance (Sartorius, Göttingen, Germany) with an accuracy of 0.001 mg. The platforms were inserted into the graphite tubes using a SSA 600 solid autosampler (Analytik Jena). High purity argon (99.999%, White Martins, Sertãozinho, Brazil) was used as the purge and protection gas. The graphite furnace heating programs for the determination of Co, Ni, and Fe are presented in Table I.

A PerkinElmer® AAnalyst™100 line source flame atomic absorption spectrometer (PerkinElmer, Inc., Shelton, CT, USA), equipped with a deuterium-lamp background correction system, was used as the comparative technique. Hollow cathode lamps for Co, Fe, and Ni were operated at the 25, 30, and 25 mA current, respectively. Absorbance measurements at 240.7 nm (Co), 248.3 nm (Fe), and 232.0 nm (Ni) using a 3-s integration time and 0.2 nm spectral bandwidth were used. Air and acetylene flow rates for all elements were established at a proportion of 4:2 oxidant/fuel. The aspiration flow rate and observation height were fixed at 5.0 mL min^{-1} and 7 mm, respectively.

An Anton Paar Multiwave® microwave oven (Graz, Austria), equipped with six Teflon® flasks, was used for sample digestion.

Reagents, Standards, and Samples

All solutions were prepared using high purity water (18.2 MΩ–cm resistivity) obtained from a Rios 5® reverse osmosis system and a Milli-Q® Academic® deionizer (Millipore Corporation, Bedford, NY, USA). Suprapur® nitric acid (Merck Darmstadt, Germany) was used for preparing the solutions. Hydrofluoric acid (Merck, Darmstadt, Germany) and hydrogen peroxide (Panreac, Barcelona, Spain) were used for wet digestion.

Working standard solutions containing 0.1 mg L^{-1} Co, 1.0 mg L^{-1} Fe and Ni were prepared by proper dilution of 1000 mg L^{-1} Co, Fe, and Ni single stock standards (Specsol, São Paulo, Brazil) and acidified to 0.1% (v/v) HNO_3.

For LS FAAS analysis, calibration curves in the range of 0.1–4.0 mg L^{-1} Co, Fe, and Ni were prepared daily by properly dilution of the standard solutions.

Solar- and electronic-grade silicons were furnished by the laboratory of metallurgical processes of the Instituto de Pesquisas Tecnológicas do Estado de São Paulo (IPT) (São Paulo, Brazil). The samples were pulverized by scraping the silicon piece with a silicon carbide spatula. Accuracy was assessed by addition/recovery tests with 99% SiO_2, 0.5-10 µm (Sigma-Aldrich, USA).

For comparative purposes, the SoG-Si and EG-Si samples were digested according to the following procedure: a mass of 0.2 g of sam-

TABLE I
Optimized Heating Program for the Determination of Co, Fe, and Ni in SoG-Si by HR-CS GFAAS

Step	Temperature (°C)	Ramp (°C s^{-1})	Hold Time (s)	Argon Flow Rate (L min^{-1})
Drying 1	110	10	10	2.0
Drying 2	130	5	10	2.0
Pyrolysis	1600[a], 1300[b]	50	15	2.0
Auto-zero*	1600[a], 1300[b]	0	5	0
Atomization	2400[a], 2650[b]	2400[a], 3000[b]	6[a], 10[b]	0
Cleaning	2600[a], 2700[b]	500	5	2.0

* Step to ensure that the atomization starts without the presence of argon.
[a] Conditions for Co; [b] Conditions for Fe and Ni determinations.

ples was accurately weighed and transferred to the microwave flasks, followed by addition of 3.0 mL of concentrated nitric acid, 2.0 mL of concentrated hydrofluoric acid, and 1.0 mL of hydrogen peroxide. Then the optimized program of the microwave oven was run using (a) 15 minutes from 0 to 700 W; (b) 15 minutes from 700 to 900 W; (c) 15 minutes at 900 W; and (d) 20 minutes at 0 W (ventilation). After digestion, the resulting solutions were transferred to digestion tubes and heated for 3 hours at 150 °C in the digestion heating block in order to eliminate the hydrofluoric acid. After cooling, the sample digests were transferred to 25-mL volumetric flasks and made up to volume using distilled deionized water. The samples were digested in triplicate.

All glasses and polypropylene vessels were washed with Extran® detergent, soaked in 10% (v/v) HNO_3 for 24 hours, then rinsed abundantly with deionized water before use.

Analytical Procedure

The thermal behavior of the analytes was evaluated in a multivariate experiment using a factorial design 2^n, where n is the number of variables. In this work, a full 2^3 factorial design was employed, the variables evaluated were the pyrolysis and atomization temperatures and the sample size. These variables were evaluated in two levels, minimum (–) and maximum (+). Table II lists the experimental matrix used for optimization, together with the minimum and maximum levels of each evaluated variable for Co, Fe, and Ni.

The experimental data obtained from the factorial design were processed using the software Statgraphics Centurion XVI (Statpoint Technologies, Warrenton, VA, USA), generating a mathematical function whose maximization corresponded to the ideal analytical conditions for each analyte (or for the joint monitoring of the analytes). The values of the three variables optimized by the factorial design were used in the graphite furnace heating program in subsequent experiments.

After establishing the heating programs, analytical curves were constructed in the 0.0–2.0 ng Co, 0.0–15.0 ng Fe, and 0.0–3.5 ng Ni mass ranges, which were obtained by delivering different aliquots of 0.1 mg L^{-1} Co, 1.0 mg L^{-1} Fe and Ni standard solutions. The first point of the calibration curves, corresponding to 0.0 ng (blank), was obtained by measuring the absorbance with an empty platform (concept of zero mass).

The possibility of using calibration with aqueous standards for direct solid sample analysis was evaluated by means of multiple effects of matrices by comparing the characteristic masses (m_0) and slopes of the calibration curves built up in 0.1% (v/v) HNO_3 and SiO_2 media spiked with the analytes.

Accuracy was evaluated by means of addition/recovery tests. Masses of 0.15 mg SiO_2 were spiked with 5.0 and 10.0 µL of 0.1 mg L^{-1} Co, 3.0 and 5.0 µL of 1.0 mg L^{-1} Fe and Ni standard solutions in order to obtain final concentrations of 3.3 mg kg^{-1} Co, 6.7 mg kg^{-1} Co, and 20 mg kg^{-1} and 33 mg kg^{-1} Fe and Ni, respectively. The precision was evaluated in terms of relative standard deviation (%RSD) obtained for three successive measurements of each sample.

The limits of detection (LOD) and quantification (LOQ) were calculated according to the IUPAC recommendation: 3 x SD^{blank}/b (LOD), and 10 x SD^{blank}/b (LOQ), where SD is the standard deviation for 10 measurements of the blank (using empty platform) and b is the slope of the calibration curve.

After optimizing the calibration conditions, methods were applied to the determination of Co, Fe, and Ni in solar- and electronic-grade silicon samples. Aliquots of aqueous standards were manually injected onto the SSA 600 platform using micropipettes. Sample amounts in the range of 0.1– 0.2 mg were manually transferred to the graphite platforms, weighed and introduced into the atomization compartment using the automated solid sampling accessory. All measurements were

TABLE II
Factorial Design (2^3) Used for Optimization of the Experimental Conditions

Experiment*	Pyrolysis Temperature (°C)	Atomization Temperature (°C)	Sample Mass (mg)
1	+ (1600[a],1500[b])	+ (2600[a], 2650[b])	+ (0.3–0.4[a], 0.2–0.3[b])
2	+ (1600[a],1500[b])	+ (2600[a], 2650[b])	- (0.1–0.2)
3	+ (1600[a],1500[b])	- (2400[a], 2500[b])	+ (0.3–0.4[a], 0.2–0.3[b])
4	+ (1600[a],1500[b])	- (2400[a], 2500[b])	- (0.1–0.2)
5	- (1400[a],1300[b])	+ (2600[a], 2650[b])	+ (0.3–0.4[a], 0.2–0.3[b])
6	- (1400[a],1300[b])	+ (2600[a], 2650[b])	- (0.1–0.2)
7	- (1400[a],1300[b])	- (2400[a], 2500[b])	+ (0.3–0.4[a], 0.2–0.3[b])
8	- (1400[a],1300[b])	- (2400[a], 2500[b])	- (0.1–0.2)

* n=3.
[a] Conditions for Co.
[b] Conditions for Fe and Ni.

carried out in triplicate (n=3), and the integrated peak absorbance was equivalent to 3 pixels.

For LS FAAS, the sample digests were properly diluted in order to adjust the measured absorbance in the linear working range. All measurements were carried out in triplicate.

RESULTS AND DISCUSSION

Thermal Behavior of Analytes and Heating Program of Atomizer

The presence of metal contaminants in solar-grade silicon and electronic-grade silicon (e.g., Co, Fe, and Ni) may reduce the efficiency of silicon chips used in most electronic equipment. First, measurements employing the most sensitive lines of the analytes showed absorbance exceeding the linear working ranges, suggesting alternative lines with lower sensitivities should be used. The line of Co at 252.136 nm (37% relative sensitivity) and the lines of Fe and Ni at 305.909 nm (4% relative sensitivity) and 305.764 nm (3.3% relative sensitivity) were selected for further experiments. It should be noted that Fe and Ni were simultaneously monitored because their lines are in the same spectral window of the spectrometer. Shown in Figure 1 are the spectra recorded for Co (Figure 1a) and Fe and Ni (Figure 1b) in a sample of solar-grade silicon.

After selecting the suitable analytical lines, the heating program of the graphite furnace was optimized in order to maximize the matrix removal and to calibrate with aqueous standards for solid sample analysis. For the evaluation of the thermal behavior of Co, Fe, and Ni, the maximum and minimum levels of the multivariate experiment were chosen after considering the data published in earlier publications (22–24) and using the conditions as recommended by the manufacturer.

The use of the factorial design may reduce the number of experiments required for establishing the optimum conditions in order to observe further interactions among the variables which are not possible in a univariate mode. The obtained experimental responses for each condition were used for generating a mathematical model and evaluating the influence of the variables on the absorbance signals. For the selected intervals, no significant variation in the Co absorbance was observed at the 95% confidence level when the pyrolysis and atomization temperatures were varied. Higher analytical signals were observed for increased sample sizes. The optimum conditions for the pyrolysis and atomization temperatures were 1600 °C and 2400 °C, respectively; and for sample mass it was 0.1–0.2 mg.

For Fe and Ni, the simultaneous monitoring of both elements was considered for selecting the optimum analytical signals. A significant increase on the Fe response was observed by increasing the atomization and pyrolysis temperatures, and also for the interactions: (a) pyrolysis and atomization temperatures; (b) pyrolysis temperature and sample size; (c) pyrolysis temperature, atomization temperature and sample size. Similarly to Co, no significant variation in the Ni absorbance was observed at the 95% confidence level in the intervals evaluated for variables. This may be due to the more refractory characteristics of these elements in comparison to Fe. The optimum conditions found were 1300 °C pyrolysis temperature, 2650 °C atomization temperature, and 0.1- 0.2 mg sample size. These conditions were employed for further experiments.

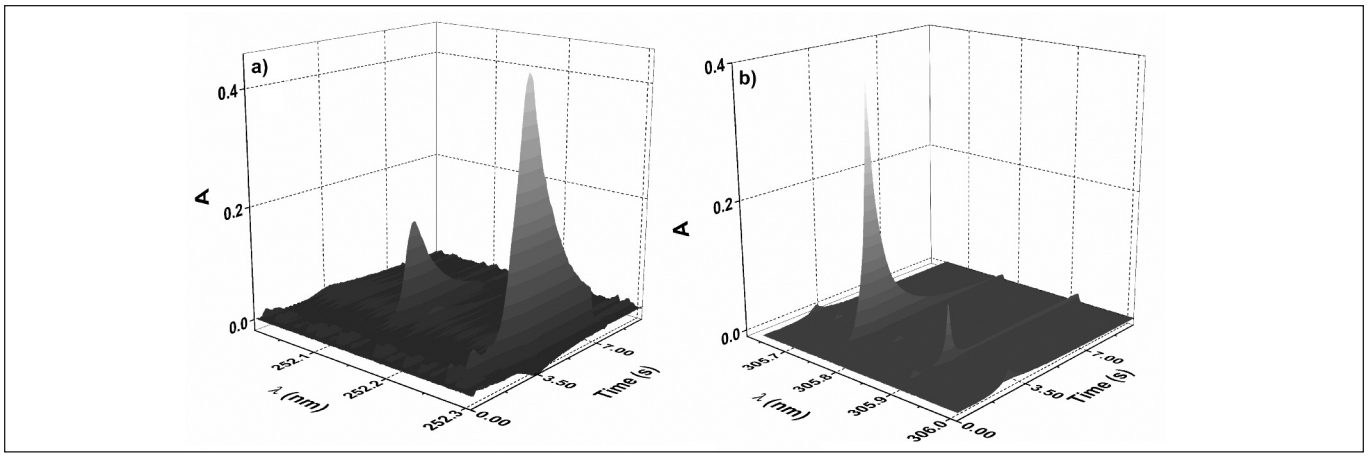

Fig. 1. Time-resolved spectra of Co in the vicinity of line at 252.136 nm (a) and (b) Ni (305.909 nm) and Fe (305.760 nm) lines in SoG-Si.

Matrix Effects

Matrix effects were evaluated by comparing the slopes of the calibration curves (0.0–2.0 ng Co, 0.0– 15.0 ng Fe, and 0.0–3.5 ng Ni) built up in aqueous solution and solid media (SoG-Si). For this sequence, good linear correlation coefficients (r) were obtained for Co (0.9999, 0.9968), Fe (0.9959, 0.9967), and for Ni (0.9977, 0.9955); and the slopes of the analytical curves were 0.22745, 0.21372 (Co), 0.03791, 0.03812 (Fe), and 0.0217and 0.0206 (Ni) for aqueous and solid calibration, respectively. These data expect errors of < 6.0%, 1.6%, and 5.3% for Co, Fe, and Ni, respectively, when aqueous standard calibration is used for analysis of the solid samples. The characteristic masses calculated for aqueous and solid media, respectively, were 0.0195 pg and 0.0199 pg (Co); 0.094 pg and 0.086 pg (Fe), and 0.53 pg and 0.54 pg (Ni). Matrix matching or analyte addition calibrations would minimize matrix effects. However, taking into consideration that errors of < 6% are acceptable for solid sample analysis, aqueous calibration is straightforward and was adopted for further studies.

Analytical Performance

The main figures of merit relating to the direct determination of Co, Fe, and Ni in solar- and electronic-grade silicon were evaluated. A 0.10–0.20 mg quantity of sample was weighed and assayed. The calculated characteristic masses calculated for aqueous and solid media were 0.0195 pg and 0.0199 pg (Co); 0.094 pg and 0.086 pg (Fe), and 0.53 pg and 0.54 pg (Ni). The limit of detection, calculated according to IUPAC recommendation, was 0.39 mg kg^{-1}, 1.14 mg kg^{-1}, and 5.71 mg kg^{-1} for Co, Fe, and Ni, respectively. For comparison purposes, the samples were digested and analyzed by LS FAAS. The values for Co, Fe, and Ni obtained by both techniques (Table III) were in agreement at the 95% confidence level (paired *t*-test). Also, accuracy was checked by addition/recovery tests. Cobalt, Fe, and Ni were determined in high-purity silica spiked with 3.3 and 6.6 mg kg^{-1} Co, 20 and 33 mg kg^{-1} Fe and Ni. Recoveries were in the range of 94–97% (Co), 87–109% (Fe), and 88–99% (Ni). The found values were in agreement with the spike values for Co, Fe, and Ni at the 95% confidence level. The method was then applied for Co, Fe, and Ni determination in solar- and electronic-grade silicon samples. The analysis of the samples showed concentrations in the range of 7.8–16.5 mg kg^{-1} for Co, 28.0–36.2 mg kg^{-1} for Fe, and 228–355 mg kg^{-1} for Ni. The relative standard deviation (n=12) for a sample containing 7.80 mg kg^{-1} Co, 36.2 mg kg^{-1} Fe, and 228.5 mg kg^{-1} Ni was 6.4% for Co, 6.1% for Fe, and 1.0% for Ni. The main figures of merit for the determination of Co, Fe, and Ni in pure silicon by the proposed SS HR-CS GFAAS methods are depicted in Table IV.

TABLE III
Results (mean ± standard deviation) for Co, Fe, and Ni (mg kg^{-1}) Determined (n=3) in SoG-Si and EG-Si by Proposed DSS HR-CS GFAAS and LS FAAS Comparatve Technique

Analyte	SoG-Si		EG-Si	
	DSS HR-CS GFAAS	LS FAAS	DSS HR-CS GFAAS	LS FAAS
Co	7.80 ± 0.50	8.58 ± 0.62	16.5 ± 1.2	16.4 ± 1.3
Fe	36.2 ± 2.2	37.9 ± 1.9	28.0 ± 2.7	27.5 ± 0.8
Ni	228.5 ± 2.2	233.7 ± 5.9	355.0 ± 28.8	329.1 ± 23.0

TABLE IV
Main Figures of Merit for the Determination of Co, Fe, and Ni in Pure Silicon by Proposed Method Based on DSS HR-CS GFAAS

Parameters	Co	Fe	Ni
LOD (mg kg^{-1})	0.39	1.14	5.71
LOQ (mg kg^{-1})	1.30	3.80	19.0
m_0 (pg)	0.0195 (aqueous); 0.0199 (solid)	0.094 (aqueous); 0.086 (solid)	0.53 (aqueous); 0.54 (solid)
RSD (%)	6.0	1.6	5.3
b	0.22745(aqueous); 0.21372 (solid)	0.03791(aqueous); 0.03812 (solid)	0.0217(aqueous); 0.0206 (solid)
r	0.9999 (aqueous); 0.9968 (solid)	0.9959 (aqueous); 0.9967 (solid)	0.9977 (aqueous); 0.9955 (solid)
Pyrolysis Temperature (°C)	1600	1300	1300
Atomization Temperature (°C)	2400	2650	2650
Sample Mass (mg)	0.1–0.2	0.1–0.2	0.1–0.2
Modifier	No	No	No

LOD: limit of detection; LOQ: limit of quantification; m_0: characteristic mass; RSD: relative standard derivation; b: slope; r: correlation coefficient.

CONCLUSION

The determination of contaminants in a silicon matrix is an analytical challenge due to the difficulties and complexities of sample preparation. The heating program and sample size were optimized by using a factorial design which reduces the number of experiments and enables the consideration of interactions between the variables. Sample concentrations ranged between 7.8–16.5 mg kg^{-1} (Co); 28.0–36.2 mg kg^{-1} (Fe), and 228–355 mg kg^{-1} (Ni). Cobalt, Fe, and Ni were precisely and accurately determined. The employment of HR-CS GFAAS combined with solid sampling allows the determination of the analytes in high-purity silicon without any previous sample preparation and addition of reagents.

ACKNOWLEDGMENT

The authors would like to thank the Fundação de Amparo à Pesquisa do Estado de São Paulo for financial support of this work (Grant #2014/12595-1). The authors are also grateful to the Coordenação de Aperfeiçoamento de Pessoal de Nível Superior (CAPES) for fellowships to D.V.B. and to the Conselho Nacional de Desenvolvimento Científico e Tecnológico (CNPq) for fellowships to A.I.B. and M.A.B., and researchship to J.A.G.N.

Received Novemvee 7, 2016.

REFERENCES

1. K.H. Solangi, M.R. Islam, R. Saidur, N.A. Rahim, H. Fayaz, Renew. Sustain. Energy Rev. 15, 2149 (2011).
2. G.R. Timilsina, L. Kurdgelashvili, P.A. Narbel, Renew. Sustain. Energy Rev. 16, 449 (2012).
3. M. Hystad, C. Modanese, M. Di Sabatino, L. Arnberg, Sol. Energy Mater. Sol. Cells 103, 140 (2012).
4. Y. Delannoy, J. Cryst. Growth 7, 360 (2012).
5. G. Coletti, P.C.P. Bronsveld, G. Hahn, W. Warta, D. Macdonald, B. Ceccaroli, Adv. Funct. Mater. 21, 879 (2011).
6. S. Meyer, S. Wahl, A. Molchanov, K. Neckermann, C. Moller, K. Lauer, Sol. Energy Mater. Sol. Cells 130, 668 (2014).
7. G. Kolosovska, A. Viksna, G. Chikvaidze, A. Osite, A. Opalais, Mater. Sci. Eng. 38, 1 (2012).
8. C. Bendicho, I. Lavilla, F. Pena-Pereira, V. Romero, J. Anal. At. Spectrom. 27, 1831 (2012).
9. J. Rip, K. Wostyn, P. Mertens, S. De Gendt, M. Claes, Energy Proced. 27, 154 (2012).
10. S. Darwiche, M. Benmansour, N. Eliezer, D. Morvan, Prog Photovoltaics Res. Appl. 20, 463 (2012).
11. M. Di Sabatino, A.L. Dons, J. Hinrichs, L. Arnberg, Spectrochim. Acta Part B 66, 144 (2011).
12. J. Hampel, F.M. Boldt, H. Gerstenberg, G. Hampel, J.V. Kratz, S. Reber, Appl. Radiat. Isto. 69, 1365 (2011).
13. P. Peres, A. Merkulov, F. Desse, M .Schuhmacher, Surf. Interface Anal. 43, 643 (2011).
14. P.L. Buldini, A. Mevoli, J.L. Sharma, Talanta 47, 203 (1998).
15. M.A. Belarra, M. Resano, F. Vanhaecke, L. Moens, TrAC Trends Anal. Chem. 21, 828 (2002).
16. B. Welz, Anal. Bioanal. Chem. 381, 69 (2005).
17. M. Resano, M. Aramendía, M.A. Belarra, J. Anal. At. Spectrom. 29, 2229 (2014).
18. A.T. Duarte, M.B. Dessuy, M.G.R. Vale, B. Welz, Anal. Methods 5, 6941 (2013).
19. S. Kelestemur, M. Özcan, Microchem. J. 118, 55 (2015).
20. A.F. da Silva, D.L.G. Borges, F.G. Lepri, B. Welz, A.J. Curtius, U. Heitmann, Anal. Bioanal. Chem. 382, 1835 (2005).
21 M. Resano, M.D.R. Flórez, I. Queralt, E. Marguí, Spectrochim. Acta Part B 105, 38 (2015).
22. B. Gómez-Nieto, M.J. Gismera, M.T. Sevilla, J.R. Procopio, Talanta 116, 860 (2013).
23. M. Resano, E. Bolea-Fernández, E. Mozas, M.R. Flórez, P. Grinberg, R.E. Sturgeon, J. Anal. At. Spectrom. 28, 657 (2013).
24. A.S. Ribeiro, M.A. Vieira, A.F. da Silva, D.L.G. Borges, B. Welz, U. Heitmann, Spectrochim. Acta Part B 60, 693 (2005).

Feasibility of a Fast and Green Chemistry Sample Preparation Procedure for the Determination of K and Na in Renewable Oilseed Sources by Flame Atomic Emission Spectrometry

Kamyla Cabolon Pengo[a], Vanessa Cruz Dias Peronico[a], Luiz Carlos Ferreira de Souza[b], and Jorge Luiz Raposo, Jr.[a]*

[a] Federal University of Grande Dourados, School of Exact and Technology Science, PO Box 364, 79804-970 Dourados, MS, Brazil

[b] Federal University of Grande Dourados, School of Agronomic Science, PO Box 364, 79804-970 Dourados, MS, Brazil

ABSTRACT

This work describes a fast and green chemistry procedure to determine potassium (K) and sodium (Na) in alternative oilseed crops by flame atomic emission spectrometry (FAES) using an ultrasound (US) system for sample preparation. The use of 10 mL of a 0.12 mol L^{-1} HCl solution, 10 minutes of extraction, and 25 ºC allowed the use of ≈0.1000 g of samples to extract the mineral content of the samples. The main and secondary atomic lines were evaluated, but only the secondary (404.4 nm for K and 330.3 nm for Na) provides a satisfactory (1.00–150.00 mg L^{-1} K and 1.00–120.00 mg L^{-1} Na) analytical calibration range for the determination of K and Na in a single run without need of further dilution of the samples. Recoveries of K and Na added to samples varied from 93.7–99.1% with the precision better than 3.5%. Five samples of renewable oilseeds were analyzed by FAES with the proposed sample preparation procedure using a closed-vessel microwave-assisted acid digestion for comparative purposes. The results obtained using an ultrasound sample preparation procedure were in agreement at the 95% confidence level (paired *t*-test), with those obtained by microwave-assisted digestion. The found concentrations were 6.02±0.11 – 7.75±0.47 mg g^{-1} K and 1.41±0.05 – 2.01±0.10 mg g^{-1} Na, with a precision better than 5.3%. The limit of detection was 52.45 and 73.83 µg g^{-1} for K and Na, respectively.

INTRODUCTION

Agriculture is a modern, prosperous, and highly competitive sector in Brazil, and it is considered as the propelling agent of the national economy. Among various sectors of agriculture, soybeans and sugarcane are the most important, and together with coffee and livestock they are currently the pillars of Brazil's economy (1). Although soybeans are one of the main products used in the Brazilian culture and are raw materials used for the production of vegetable oil and/or biodiesel, alternative and renewable oilseed sources are often evaluated as another effective option for these purposes. Oilseed crops require no new investment of agricultural implements, contributes to improving the crop rotation system, and can increase the farmer's income by offering competitive profits. Since there is a lack of research done about the alternative uses of oilseed crops, an investigation related to the mineral content of these oilseed crops should be performed.

Potassium and sodium are the most important elements for vegetative growth, and constitute around 10% of its dry matter (2-4). These elements are required for many metabolic processes such as osmoregulation, protein synthesis, photosynthesis, opening and closing of the stomata, soil and water absorption, enzymatic activity, and therefore monitoring of the quality of agricultural crops is essential (5-7).

The elemental determination of K and/or Na is frequently performed by spectrometric techniques (8-15). Most of these methods involve a sample pretreatment step, which can be done by converting the sample into an aqueous solution using mineral acids and thermal or radiant energy for organic matter decomposition (16-19). This is a critical step in routine analysis, but is very time-consuming, results in incomplete solubilization of the matrices, analyte losses by volatilization, contamination in the handling processes due to the interaction between analyte and bottles, and contamination of the solutions by the reagents used (16-18, 20, 21).

From this perspective, non-destructive sample pretreatment procedures, such as those employing ultrasonic waves, are an alternative to circumvent acid digestions, and can be used for extraction, solubilization, and digestion processes using an ultrasonic bath or a probe (22, 23) with diluted acids and is

Corresponding author.
E-mail: jorgejunior@ufgd.edu.br
Tel.: +55 67 34102092

performed at room temperature (23-25). The most important advantages associated with the ultrasonic waves includes: (a) reduced time required for sample preparation, (b) reduced consumption of concentrated reagents, and (c) sample preparation is simple and relatively low cost (23, 25, 26).

In this sense, this work describes the first development of a simple and robust sample preparation procedure using an ultrasonic extraction system for the determination of K and Na in renewable oilseed sources by flame emission absorption spectrometry.

EXPERIMENTAL

Instrumentation

The measurements were carried out using a Varian 240FS flame atomic absorption spectrometer (Agilent Technologies®, Mulgrave, Victoria, Australia) operating in emission mode. The instrumental operating parameters are listed in Table I. High-purity acetylene (99.7% White Martins, Dourados, Brazil) was used as fuel, and an air-acetylene flame was used for atomization of K and Na.

A 515 Orion (Fanem®, São Paulo, SP, Brazil) forced air oven and a TE-361 (Tecnal®, Piracicaba, SP, Brazil) stainless steel mill were used to dry and powder the oilseed samples, respectively. A Unique USC-14004 (Unique®, Indaiatuba, SP, Brazil) ultrasonic bath, operating at 40 kHz, was used to leach the element from the oilseed samples. An Excelsa™ 206 BL (Fanem®, São Paulo, SP, Brazil) centrifuge was used to separate the solid and liquid phases. A Multiwave® 3000 microwave oven (Anton Paar, Graz, Austria) was used as a comparative sample preparation procedure which employed acid digestion of the samples.

Reagents and Analytical Solutions

High purity deionized water obtained from a Milli-Q® Plus reverse osmosis system (resistivity 18.2 MΩ-cm, Millipore Corporation, Bedford, MA, USA) was used to prepare all solutions. Nitric acid [65% (v/v), Sigma-Aldrich®, St. Louis, MO, USA] was used to prepare all analytical solutions, to optimize the extracting acid solutions, and for the microwave-assisted acid digestion. Hydrochloric acid [37% (v/v), Sigma-Aldrich®, St. Louis, MO, USA] was used as the extracting acid solution. A 150.000 mg L^{-1} Cs solution was prepared by dissolving 9.56 g CsCl [99.5% purity, Sigma-Aldrich®, St. Louis, MO, USA) with deionized water, followed by adding 1.5 mL HNO_3, and dilution to 50 mL using deionized water.

Different dilute hydrochloric acid solutions (0.012, 0.120, and 1.200 mol L^{-1}) were prepared for the evaluation of the effect of the acid concentration of the extraction solution on the ultrasonic-assisted extraction.

Analytical solutions containing 1.00 – 150.0 mg L^{-1} K and 1.00 – 120.0 mg L^{-1} Na were prepared daily using appropriate dilution of 1000 mg L^{-1} single-element standard stock solutions (SpecSol®, SRM-682, USA) in 1.0% (v/v) nitric acid and 1000 mg L^{-1} Cs media.

All of the solutions were stored in high-density polypropylene bottles (Nalgene®, Rochester, NY, USA). Plastic bottles and glassware were cleaned by soaking in 10% (v/v) HNO_3 for at least 24 hours, followed by thorough rinsing with deionized water before use.

Sampling and Sample Preparation

A 1000-g amount of four-months old seeds of the genus *Crambe abyssinica Hochst, Guizotia abyssinica, Brassica napus var. oleífera, Carthamus tinctorius L.*, and *Raphanus sativus L. var. oleiferus Metzg* renewable oilseed sources were randomly collected during the 2014 harvest time from five different areas (15 x 30 m) located in the Experimental Farm of the Agricultural Sciences (22º 14'S and 54º 49'W), which is situated 8 km from the Federal University of Grande Dourados (Dourados, MS, Brazil). The samples of each species were stored in individually labeled paper bags, and then transported to the laboratory. The seeds were separately and thoroughly washed with tap water and then with deionized water. A 10.0-g subsample of each oilseed sample was dried at 80 ºC for 120 hours in a forced air oven, ground in a stainless steel mill, and then sieved using a No. 20 sieve (0.84 mm opening size).

TABLE I
FAES Instrumental Operations Conditions for the Determination of Na and K

Instrumental Conditions	K	Na
Working range (mg L^{-1})	1.00 – 150.00	1.00 – 120.00
Wavelength (nm)	404.4	330.3
Burner head (mm)	100	
Air flow rate (L min^{-1})	13.0	
Acetylene flow rate (L min^{-1})	2.0	
Slit width (nm)	0.5	

A 0.1000-g portion of pretreated sample was accurately weighed (± 0.0001 g) and transferred to a 50-mL polypropylene flask, followed by addition of 15 mL acid leaching solution. The mixtures were subjected to an ultrasound energy corresponding to 40 kHz for 30 seconds to leach the elements from the seeds into the acid solution. After sonication, the acid extracts obtained were separated from the remaining solid materials using centrifugation for 5 minutes at 4000 rpm, followed by filtration into 25-mL polypropylene flasks. All of the acid leaching solutions (samples and blanks) were prepared in 1000 mg L^{-1} Cs. Three replicates of each alternative oilseed sample and blank were used to optimize the analytical parameters of the extraction procedure. All of the measurements were performed using five replicates.

For comparative purposes, the alternative oilseed materials were also mineralized in a closed-vessel microwave-assisted digestion procedure. For microwave digestion, an accurately weighed 0.1000-g sample was transferred into a microwave flask, followed by addition of 6.0 mL of HNO_3 and 2.0 mL of deionized water. The optimized heating program is listed in Table II. After digestion and cooling, the resulting solutions obtained were transferred into 25-mL volumetric flasks, and brought to volume with deionized water in 1000 mg L^{-1} Cs media. Three sample replicates were used for microwave-assisted acid decompositions.

Ultrasonic (US) Extraction Conditions and Measurement Procedure

The influence of the extracting solution (acid, concentration, and volume), sample mass, and sonication time on the sensitivity for K and Na was investigated using PIATV 02/2010 Soybean reference material (0.84 mm particle size) obtained from Embrapa Agropecuária Oeste (Dourados, MS, Brazil) by varying the acid solution [HNO_3, HCl or HNO_3:HCl (1:1, v/v)], concentration (0.012, 0.120 and 1.200 mol L^{-1}), the volume of the extracting solution (7.5, 10.0 and 15.0 mL), sample mass (0.1000, 0.2500 and 0.5000 g), and the sonication time (30, 60, 120 and 180 seconds). Due to the absence of Na in PIATV 02/2010, an aliquot of 1000 mg L^{-1} Na standard solution was added to the selected soybean reference material in order to achieve a 10.0-mg g^{-1} Na content.

At a 5.0-mL min^{-1} sample flow rate, the integrated emission intensity for blanks, working standard solutions, reference material extraction solution, and the sample solutions were measured at less sensitive atomic lines for K at 404.4 nm and Na at 330.3 nm under optimal instrumental conditions to obtain the calibration curve within the 1.00 – 150.0 mg L^{-1} K and 1.00 – 120.0 mg L^{-1} Na ranges. All measurements were carried out in five replicates.

The matrix effect was checked using recovery tests for spiked samples performed at two levels by adding aliquots of the 1000 mg L^{-1} single-element standard stock solutions to all alternative oilseed samples before the extraction procedure to obtain extracts with 25.0 and 50.0 mg L^{-1} of K and Na. The limit of detection (LOD) and limit of quantification (LOQ) were calculated according to the IUPAC recommendation (27). Statistical tests used in the data processing (mean, standard deviation, and precision) were done using the Microcal OriginPro® 8.0 program and Microsoft® Office Excel® 2007.

RESULTS AND DISCUSSION

Analytical Features for Determining K and Na

Whereas the content of macronutrients in plants is typically in the order of mg g^{-1} (14, 28), the determination of K or Na by line source flame atomic emission spectrometry (LS-FAES) in one run is not feasible if the most sensitive analytical lines (766.5 nm for K or 589.0 nm for Na) are used due to the limited linear calibration interval (29). For K and/or Na concentrations higher than the upper limit of the linear response of the calibration plots built up using the most sensitive analytical lines, the secondary line for K at 404.4 nm or Na at 330.3 nm might be employed to circumvent this problem. The use of a less sensitive atomic line is a better way to reduce sensitivity for determining major elements and to avoid further dilution of the sample solutions. At 5.0 mL min^{-1} of sample flow rate and 100 mm burner opening (standard air/acetylene burner head), the influence of the ratio of air-acetylene flow rates (0.138, 0.146, 0.154, 0.162, and 0.169) on emission intensity of K and Na was evaluated using 1.0 mg L^{-1} at 766.5 nm (K) and 589.0 nm (Na), and 10.0 mg L^{-1} at 404.4 nm (K) and 330.3 nm (Na). For this, different fuel-oxidant ratios were obtained by changing the flow rate

TABLE II
Microwave-Assisted Digestion Heating Program for Renewable Oilseed Samples

Step	T_{ramp} (min)	T_{hold} (min)	Power (W)	T (°C)
1	10	5	600	120
2	15	10	1000	200
3	0	15	0	Ventilation

of acetylene from 1.8 to 2.2 L min^{-1} and fixing the air flow rate at 13.0 L min^{-1}. The best situations achieved for flame composition for all wavelengths studied was 2.0 L min^{-1} of acetylene. Under the established conditions of the 240FS equipment, the linear working range at 766.5 and 404.4 nm for K and 589.0 and 330.3 nm for Na was evaluated by plotting curves of emission intensity versus K or Na concentration within the 0.10 – 150.00 mg L^{-1} intervals. The calibration plots in the 0.10 – 150.00 mg L^{-1} intervals provide calibration curves only up to 4.00 mg L^{-1} at 766.5 nm for K, and up to 2.00 mg L^{-1} at 589.0 nm for Na. However, the less sensitive analytical atomic lines provide calibration plots up to 150 mg L^{-1} K and 120 mg L^{-1} Na, with typical linear correlation coefficients better than 0.9980 for K and 0.9992 for Na. The main figures of merit for the K and Na atomic lines are shown in Table III.

Analysis of Table III reveals that the highest sensitivity, as seen by the slopes, are 0.2463 K and 0.1718 Na. Lower limits of detection were pbtained with the main atomic line, however, with a narrow (0.50–4.00 mg L^{-1} K and 0.50–2.00 mg L^{-1} Na) linear working range and perhaps insufficient for determining high concentrations of K and Na. In this case, where the content of the analyte in the sample digests and/or extracts is naturally above the linear range of calibration for 766.5 nm (K) and 589.0 nm (Na), the alternate atomic line at 404.4 nm (K) and 330.3 nm (Na) can be used to determine K and Na in the selected samples. The use of secondary and less sensitive (0.0063-K and 0.0061-Na slopes) atomic lines allowed extending the linear calibration range up to 150.0 mg L^{-1} K and 120.0 mg L^{-1} Na with a satisfactory limit of detection (0.2098 mg L^{-1} K and 0.2956 mg L^{-1} Na) and low relative standard deviation (< 2.4%), suggesting that the secondary line gives precise measurements. Then, the 404.4 nm for K and 330.3 nm for Na atomic lines were used to optimize the US procedure, to validate the methodology, and to determine the elements by FAES.

Optimization of Ultrasound-assisted Extraction Procedure

Nitric and/or hydrochloric acid are often reported in studies involving extraction of the inorganic species using non-destructive sample preparation procedures (30, 31); however, acid mixtures have also been reported (32). In this sense, different acid solutions [HCl, HNO_3 and HCl:HNO_3 (1:1)] at 1.00 mol L^{-1} were evaluated to check the effectiveness of these solutions for leaching K and Na from PIATV 02/2010 reference material. The influence of these different acid solutions was determined using univariate analysis by fixing the solution volume (10 mL), sonication time (180 seconds), sample mass (0.2500 g), and bath temperature at 25 ºC. The results obtained are shown in Table IV.

It can be seen in Table IV that unsatisfactory recoveries were obtained with 1.00 mol L^{-1} HNO_3 (67% for K and 62% for Na) or HCl:HNO_3 (≈76% for K and ≈69% for Na) solutions. However, in both cases the relative standard deviations (%RSD) were < 4.6%. Only for 1.00 mol L^{-1} HCl solution the recovery (89% for K and 83% for Na) can be acceptable and produced RSD of < 2.5%. It is important to note that for a 1.00-mol L^{-1} HCl solution, the recovery was 89% for K (6.50 ± 0.14 mg g^{-1}) and 83% for Na (8.30 ± 0.21 mg g^{-1}). This value is statistically different at the 95% confidence level (paired *t*-test) with those obtained for 1.00 mol L^{-1} HNO_3 or HCl:HNO_3 solutions. By the way, alternative acid mixtures, such as *aqua regia* [3:1 (v/v)] HCl:HNO_3 and HCl:HNO_3 [1:3 (v/v)] at 1.00 mol L^{-1} were also investigated for the extraction procedure. In both cases the results were no better than those obtained using 1.00 mol L^{-1} HCl:HNO_3 [1:1 (v/v)] solution. According to the results presented in Table IV, the remaining study was performed using HCl solution.

In sample preparation using ultrasound-assisted extraction, diluted acid solutions are widely employed as extracting solvent/solution to leach out as much analyte content as possible without destroying the sample matrix by means of minimum amount of selected acids (26, 33). Using the acid solution chosen previously, different concentrations of hydrochloric acid (0.012, 0.120,

TABLE III
Figures of Merit of Main and Secondary Atomic Lines for K and Na by FAES

Element	Wavelength (nm)	Calibration (mg L^{-1})	Slope	R[c]	LOD[d] (µg L^{-1})	RSD (%)
K	766.5[a]	0.50–4.00	0.2463	0.9989	9.61	3.5
	404.4[b]	1.00–150.00	0.0063	0.9980	209.80	0.9
Na	589.0[a]	0.50–2.00	0.1718	0.9991	15.55	1.9
	330.3[b]	1.00–120.00	0.0061	0.9992	295.30	2.4

[a] Main atomic line.
[b] Secondary atomic line.
[c] Linear correlation coefficient.
[d] Limit of detection.

and 1.200 mol L^{-1}) were prepared to evaluate their performance. The influence of these HCl solutions on the K and Na recoveries were done by fixing the solution volume (10 mL), sonication time (180 seconds), sample mass (0.2500 g), and bath temperature (25 °C). The results obtained for these solutions are listed in Table IV.

A significant improvement was observed in the recoveries from the 0.012 to 0.120 mol L^{-1} HCl. While the 0.012 mol L^{-1} HCl solution can leach only 77% K (5.62 ± 0.15 mg L^{-1} of 7.30 mg g^{-1}) and 70% Na (7.00 ± 0.24 mg L^{-1} of 10.0 mg g^{-1}) from the PIATV 02/2010 reference material, the 0.120 and 1.200 mol L^{-1} HCl solutions obtained 91 and 90% recoveries for K and 84 and 86% recoveries for Na, respectively, with a relative standard deviation of < 2.7%. A paired *t*-test, at the 95% confidence level, was performed and the results showed a difference between 0.120 and 1.200 mol L^{-1} with the 0.012 mol L^{-1} HCl solutions. Based on the satisfactory recoveries obtained using 0.120 and 1.200 mol L^{-1} HCl and due to a green chemistry principle, a 0.120 mol L^{-1} HCl was adopted for further study.

Some studies report that small sample masses (high dilutions) could produce low sensitivity and poor precision/accuracy of the analyte measures due to the inhomogeneity of the sample mass of the solid-liquid extracting solution (34-36). In this sense, the increase of the mass of solid materials (sample) can improve the limits of detection and quantification due to the transference of higher contents of the analyte into the liquid phase (37). Taking this into account, portions of 0.1000, 0.2500, and 0.5000 g oilseed sample were evaluated to determine the satisfactory sample mass that produces the best recovery of K and Na. Potassium and Na recoveries using 0.1000 – 0.5000 g of the PIATV 02/2010 reference material were obtained by using 0.120 mg L^{-1} HCl and fixing the solution volume (10 mL), sonication time (180 seconds), and bath temperature (25 °C). The results described in Table IV reveal no significant influence at 95% confidence level (paired *t*-test), of sample mass up to 0.5000 g, and in all cases, the relative standard deviation was < 2.1%. Since no significant differences can be observed for the determination of K and Na using 0.1000 – 0.5000 g, an amount of 0.1000 g was used for further work.

It is important to mention that particle size also plays an important role in the extraction process (38-41), and this was one of the parameters that was evaluated to achieve the best conditions of the extraction procedure. Since PIATV 02/2010 reference material was ground to 0.84 mm (20 mesh) particle size, and the results obtained were 91% (K) and 84% (Na) recovery, it is possible to conclude that particle size does not have a significant influence on the extraction efficiency for these kinds of samples.

TABLE IV
Recovery (Mean ± Standard Deviation, n= 3) of K and Na from PIATV 02/2010 Reference Material on the Optimization of the Ultrasound-Assisted Extraction Conditions

US Extraction Conditions		K Recovery (%)	K RSD (%)	Na Recovery (%)	Na RSD (%)
Extracting Solution	HCl	89	2.2	83	2.5
	HNO_3	67	3.7	62	4.6
	HCl:HNO_3 [1:1(v/v)]	76	3.0	69	4.0
HCl Solution (mol L^{-1})	0.012	77	2.7	70	3.4
	0.120	91	1.9	84	2.7
	1.200	90	1.6	86	2.3
Sample Mass (g)	0.1000	91	1.6	84	1.9
	0.2500	93	1.7	85	2.1
	0.5000	92	1.2	87	2.0
Volume (mL)	7.50	80	4.1	78	3.5
	10.00	92	2.0	86	1.7
	15.00	98	2.7	95	2.2
Sonication Time (s)	30	98	1.9	95	2.1
	60	97	1.4	94	2.0
	120	99	0.9	94	1.9
	180	99	1.1	95	1.5

K: 7.30 ± 0.67 mg g^{-1}, Na: 10.0 mg g^{-1}

For solid-liquid extraction of metals from solid matrices using ultrasound-assisted extraction, different volumes of extracting solutions have been employed (39, 42, 43). In this work, 7.5, 10.0, and 15.0 mL of 1.0 mol L^{-1} HCl were applied to evaluate the recoveries. The analytical results are shown in Table IV. The influence of the extraction volume on extraction efficiency was significant from 7.5 to 15.0 mL, and the recovery obtained for 7.5 mL (80.0% for K and 78.0% for Na) was statistically different, at a 95% confidence level (paired *t*-test), with those obtained for 15.0 mL (98% for K and 95.0% for Na). Thus, 15.0 mL of 0.120 mol L^{-1} HCl was chosen for the optimization parameters of the ultrasound-assisted extraction procedure.

Based on the results obtained in this study (≈95% recovery), the proposed extraction procedure could be applied to determine K and Na using FAES. However, the extraction time efficiency depends on analyte-matrix interaction, extracting solution composition, and the ultrasonic system applied (26, 44). In this study, the extraction time was evaluated to reduce the time consumption of the proposed method. For this, 0.1000 g of PIATV 02/2010 reference material was subjected to 30, 60, 120, and 180 seconds sonication time under the previously optimized conditions. The results obtained are listed in Table IV.

Quantitative extractions of K (97 – 99%) and Na (94 – 95%) were obtained using 30 – 180 seconds sonication intervals with an ultrasound energy corresponding to 40 kHz. The results showed no significant difference at the 95% confidence level (paired *t*-test), and presented relative standard deviations (%RSD) from 0.9 to 1.9% (K) and 1.5 to 2.1% (Na). It is important to point out that 30 seconds of sonication is a very short and satisfactory time to extract K and Na from oilseed samples.

By using 15 mL of 0.12 mol L^{-1} HCl solution, 0.84 mm particle size, 0.1000 g sample mass, and 30 seconds sonication at 25 °C, better conditions for extracting K and Na from the selected samples were achieved. These values were adopted to validate the proposed method and for analysis of the samples.

Analysis of Oilseed Samples

Five different oilseed samples of the genus *Crambe abyssinica Hochst, Guizotia abyssinica, Brassica napus var. oleífera, Carthamus tinctorius L., and Raphanus sativus L. var. oleiferus Metzg* were submitted to the proposed extraction procedure and the final extracts were analyzed by FAES. The K and Na content, determined in the final extraction solutions, showed concentration intervals within 22.12±0.32 – 30.20±1.12 mg L^{-1} and 5.64±0.20 – 8.04±0.20 mg L^{-1}, respectively. As can be seen, only the secondary atomic line could be used for the determination of K and Na in the concentration range described above in a single run without need of further dilution of the samples. The analytical results, expressed as average values ± standard deviation (n= 3) on a dry matter basis, for the determination of K and Na in five renewable oilseed samples are listed in Table V. The analysis of the samples revealed that the concentration ranges obtained using the established ultrasound-assisted extraction procedure were in the 5.53 ± 0.08 – 7.55 ± 0.28 mg g^{-1} K and in the 1.41 ± 0.05 – 2.01 ± 0.10 mg g^{-1} Na intervals. To ensure the accuracy of the developed methodology by US, the strategies based on the addition/recovery test (using all oilseed samples) and the analysis of PIATV 02/2010 were performed. Recoveries of 97.4 ± 2.1 – 98.8 ± 3.5% K and 93.7 ± 3.3 – 99.1 ± 2.5% Na were obtained by adding an amount of K and Na as the inorganic standard at the beginning of the sample pretreatment procedure in order to achieve 25.0 and 50.0 mg L^{-1} K and Na in the final extracts.

TABLE V
Comparative Results (Mean ± Standard Deviation) of K and Na (mg g^{-1}) of the Five Renewable Oilseed Samples by FAES Using the Proposed Ultrasound-Assisted Extraction Procedure and Microwave-Assisted Acid Digestion

Oilseed Crops	Sample Preparation			
	Ultrasound-assisted Extraction		Microwave-assisted Digestion	
	K	Na	K	Na
Crambe abyssinica Hochst	7.55 ± 0.28	1.41 ± 0.05	7.73 ± 0.18	1.49 ± 0.07
Guizotia abyssinica	5.53 ± 0.14	1.84 ± 0.08	5.64 ± 0.08	1.93 ± 0.06
Raphanus sativus L. var. oleiferus Metzg	5.90 ± 0.21	1.58 ± 0.04	6.10 ± 0.15	1.55 ± 0.05
Brassica napus var. oleífera	6.07 ± 0.32	1.52 ± 0.03	6.47 ± 0.27	1.47 ± 0.04
Carthamus tinctorius L.	6.62 ± 0.16	2.01 ± 0.10	6.94 ± 0.21	2.10 ± 0.09

Finally, the results obtained for the samples using the US method were compared with those obtained using total decomposition in a closed-vessel microwave oven. The results obtained (Table V) show no significant difference at the 95% confidence level (paired *t*-test) between the values obtained for the proposed methodology and acid digestion. These results indicated that the ultrasound extraction procedure proposed in this study is free of matrix interferences. The relative standard deviation (n=12) for all measurements varied within the range of 1.8–5.3% for ultrasound-assisted extraction and 1.1–4.7% for microwave-assisted digestion.

CONCLUSION

Use of a less sensitive atomic line in FAES for K and Na was feasible for the elemental determination in a wide range of concentrations without need of further dilutions of the sample extracts, and allowed to reduce the errors associated with excessive sample handling. The methodology described offers a fast, accurate, and efficient sample preparation for the determination of K and Na in different oilseed crop samples by flame atomic emission spectrometry. In general, the proposed sample preparation makes the ultrasonic bath system advantageous as compared to acid digestion due to low time and reagent consumption, minimal generation of wastes, and therefore contributes to a green chemistry procedure.

ACKNOWLEDGMENT

The authors would like to thank the Fundação de Apoio ao Desenvolvimento do Ensino, Ciência e Tecnologia do Estado de Mato Grosso do Sul (Fundect, Process 23/200.665/2012), and the Conselho Nacional de Desenvolvimento Científico e Tecnológico (CNPq, Process n. 479186/2013-8) for their financial support of this work.

Received October 24, 2016.

REFERENCES

1. Conab, http://www.conab.gov.br/conteudos.php?a=1253&t, Last visited: 10/10/2016.
2. M. Gierth and P. Mäser, FEBS Lett. 581, 2348 (2007).
3. Z. Jianbin, H. Xiaoyan, Q. Xiaoyan, C. Shengguan, H. Yong, A.N. Umme,and Z. Guoping, J Proteomics 126, 1 (2015).
4. R.A. Leigh and R.G. Wyn Jones, New Phytol. 97, 1 (1984).
5. H. Marschner, Marschner's Mineral Nutrition of Higher Plants, Academic Press, Amsterdam, NED (2011).
6. W.T. Pettigrew, Physiol. Plantarum 133, 670 (2008).
7. F. Yang, M. Du, X. Tian, A.E. Eneji, L. Duan, and Z. Li, Field Crop Res. 163, 109 (2014).
8. M.A. Bechlin, F.M. Fortunato, R.M. Silva, E.C. Ferreira, and J.A. Gomes Neto, Spectrochim. Acta B 101, 240 (2014).
9. A.I. Barros, A.P. Oliveira, M.R.L. Magalhães, and R.D. Villa, Fuel 93, 381 (2012).
10. S.E. Dancsak, S.G. Silva, J.A. Nóbrega, B.T. Jones, and G.L Donati, Anal. Chim. Acta 806, 85 (2014).
11. A. Jesus, M.M. Silva, and M.G.R. Vale, Talanta 74, 1378 (2008).
12. A.P. Oliveira, R.D. Villa, K.C.P. Antunes, A. Magalhães, and E.C. Silva, Fuel 88, 764 (2009).
13. C.V.S. Ieggli, D. Bohrer, P.C. Nascimento, and L.M. Carvalho, Food Chem. 124, 1189 (2011).
14. S.R. Oliveira, J.L. Raposo Jr, and J.A. Gomes Neto, Spectrochim. Acta B 64, 593 (2009).
15. S.R. Oliveira, J.A. Gomes Neto, J.A. Nóbrega, and B.T. Jones, Spectrochim. Acta B 65, 316 (2010).
16. R. Anderson, Sample pretreatment and separation, London, ENG, UK (1987).
17. F.J. Holler, S.R. Crouch, and D.A. Skoog, Principles of Instrumental Analysis, Philadelphia, PA, USA (2009).
18. F.J. Krug, Métodos de preparo de amostras fundamentos sobre preparo de amostras orgânicas e inorgânicas para análise elementar. Piracicaba, SP, Brazil (2008).
19. A.I. Vogel, and G.H. Jeffery, Vogel's textbook of quantitative chemical analysis. New York, NY, USA (1989).
20. M. Hoenig, Talanta 54, 1021 (2001).
21. G. Knapp, TrAC-Trend. Anal. Chem 3, 182 (1984).
22. E. de Oliveira, J. Brazil Chem. Soc. 14, 174 (2003).
23. C.C. Nascentes, M. Korn, C.S. Sousa, and M.A.Z. Arruda, J. Brazil. Chem. Soc. 12, 57 (2001b).
24. N. Manutsewee, W. Aeungmaitrepirom, P. Varanusupakul, and A. Imyim, Food Chem. 101, 817 (2007).
25. F. Priego-Capote, and M.D. Luque De Castro, TrAC-Trend Anal. Chem. 23, 644 (2004).
26. F. Priego-Capote, and M.D. Luque De Castro, J. Biochem. Bioph. Meth. 70, 299 (2007).
27. L.A. Currie, Anal. Chim. Acta 391, 105 (1999).
28. M.E. Farago, Plants and the chemical elements: biochemistry, uptake, tolerance and toxicity. Weinheim, Germany (1994).
29. Agilent Technologies, Flame Atomic Absorption spectrometry – Analytical Methods, Mulgrave, VIC, Australia (2015).
30. J. Deng, X. Feng, and X.Qiu, Chem. Eng. J. 152, 177 (2009).
31. V.C.D. Peronico, and J.L. Raposo Jr, Food Chem. 196, 1287 (2016).
32. T.G. Kazi, M.K. Jamali, M.B. Arain, H.I. Afridi, N. Jalbani, R.A. Sarfraz, and R. Ansari, J. Hazard. Mater. 161, 1391 (2009).
33. A.S.N. Trindade, A.F. Dantas, D.C. Lima, S.L.C. Ferreira, and L.S.G.

Teixeira, Food Chem. 185, 145 (2015).

34. B.L. Batista, J.L. Rodrigues, V. Oliveira, and F. Barbosa, Forensic Sci. Int. 192, 88 (2009).

35. M. Costas, I. Lavilla, S. Gil, F. Pena, I. De La Calle, N. Cabaleiro, and C. Bendicho, Anal. Chim. Acta 679, 49 (2010).

36. I. De La Calle, N. Cabaleiro, I. Lavilla, and C. Bendicho, Spectrochim. Acta B 64, 874 (2009).

37. C.E.R. Paula, L.F.S. Caldas, D.M. Brum, and R.J. Cassella, J. Pharmaceut. Biomed. 74, 284 (2013).

38. J.L. Capelo, C. Maduro, and C. Vilhena, Ultrason. Sonochem. 12, 225 (2005).

39. A.V. Filgueiras, J.L. Capelo, I. Lavilla, and C.Bendicho, Talanta 53, 433 (2000).

40. J. Liao, B. Qu, D. Liu, and N. Zheng, Ultrason. Sonochem. 27, 110 (2015).

41. C.C. Nascentes, M. Korn, and M.A.Z. Arruda, Microchem. J. 69, 37 (2001a).

42. I. Lavilla, B. Perez-Cid, and C. Bendicho, Int J Environ Anal. Chem. 72, 47 (1998).

43. H. Minami, T. Honjyo, and I. Atsuya, Spectrochim. Acta B 51, 211 (1996).

44. S. Ohmori, J. Radioanal. Nucl. Chem. 84, 451 (1984).

ANY MATRIX
ANY INTERFERENCE
ANY PARTICLE SIZE

NexION 2000 ICP-MS: Triple quad power meets single quad versatility.

Trace metals in food, nanomaterials in water, impurities in everything from pills to electronic components: These are the sweet spot for the NexION® 2000 ICP-MS. Its sample introduction technology lets you run samples with up to 35% total dissolved solids. Plus, its interference removal capabilities give you the best detection limits for your application. And it delivers superior analysis times and single particle/cell detection capability – at least 10x faster than competitive systems. So the NexION 2000 ICP-MS is up to the most important challenge of all: ***Yours.***

For more information,
visit perkinelmer.com/NexION2000

NexION 2000 ICP Mass Spectrometer

PerkinElmer®
For the Better

Bringing a whole new level of performance and flexibility to elemental analysis

It's a very big breakthrough in a very compact, affordable package: The all-new Avio™ 200 ICP-OES is capable of handling the most difficult high-matrix solutions without dilution, for a whole new level of performance and flexibility. Its ease-of-use features and intuitive software make multi-element analysis as easy as single-element. And it delivers a whole host of "firsts" and "bests" – lowest argon consumption, fastest startup time (10 minutes from power on), superior sensitivity and resolution, and the widest linear range – in an amazingly small footprint. The Avio 200 system: It's the complete – and affordable – package.

For more information, visit perkinelmer.com/avio200

Avio 200 ICP-OES

PerkinElmer®
For the Better

With the new Titan MPS™ sample preparation system, we're delivering on the promise of a simple, safe, cost-effective microwave. But what really sets it apart is everything else you get with it: It's backed by PerkinElmer, the go-to resource and one-stop shop for all things atomic spectroscopy, so you can access the instruments, consumables, informatics, and expertise you need to optimize your research and your business. The Titan MPS sample preparation system: It's the microwave that's so much more.

www.perkinelmer.com/titanmps

PerkinElmer, Inc.
710 Bridgeport Avenue
Shelton, CT 06484-4794 USA
Phone: (800) 762-4000 or
(+1) 203-925-4602
www.perkinelmer.com

013351_03

PerkinElmer®
For the Better